

# Dynamics of rotating two-component Bose–Einstein condensates and its efficient computation

Yanzhi Zhang<sup>a</sup>, Weizhu Bao<sup>a,b,\*</sup>, Hailiang Li<sup>c</sup>

<sup>a</sup> *Department of Mathematics, National University of Singapore, Singapore 117543, Singapore*

<sup>b</sup> *Center for Computational Science and Engineering, National University of Singapore, Singapore 117543, Singapore*

<sup>c</sup> *Department of Mathematics, Capital Normal University, Northern Road 105, Western Ring 3, 100037, Beijing, PR China*

Received 24 May 2006; received in revised form 27 June 2007; accepted 29 June 2007

Available online 12 July 2007

Communicated by B. Sandstede

## Abstract

In this paper, we investigate the dynamics of rotating two-component Bose–Einstein condensates (BEC) based on the coupled Gross–Pitaevskii equations (CGPEs) with an angular momentum rotation term and an external driving field, and propose an efficient and accurate method for numerical simulations. We prove the conservation of the angular momentum expectation, derive the dynamic laws for the density of each component and condensate widths, and analyze the dynamics of a stationary state with its center shifted from the trap center. By formulating the CGPEs in either 2D (two-dimensional) polar coordinate or 3D cylindrical coordinate system, the angular momentum rotation term becomes a term with constant coefficients. This allows us to develop an efficient time-splitting method which is time reversible, time transverse invariant, unconditionally stable, efficient and accurate for the problem. Moreover, it conserves the total position density in the discretized level. The numerical method is applied to verify our analytical results and study the dynamics of quantized vortex lattices in rotating two-component BEC with/without an external driving field.

© 2007 Elsevier B.V. All rights reserved.

*Keywords:* Rotating two-component Bose–Einstein condensation; Coupled Gross–Pitaevskii equations; Angular momentum rotation; Condensate width; Angular momentum expectation; Quantized vortex lattice

## 1. Introduction

Since its realization in dilute bosonic atomic gases [2,14,10], Bose–Einstein condensation (BEC) has been produced and studied extensively in the laboratory [38,1,22], and has afforded an intriguing glimpse into the macroscopic quantum world [38]. Attention has been broadened to include exploration of quantized vortex states and their dynamics associated with superfluidity [34,1] and of systems of two or more condensates [22,24] since the first vortex experiment of BEC was realized in 1998 [1,34]. These are some of the key issues, in view of potential applications, in the study of quantized vortices which are well-known signatures of superfluidity [8] and the generation of bright beams of coherent matter waves (atom laser) [22,4]. The first experiment involving the interactions between multi-component BEC was performed with atoms evaporatively cooled in the  $|F = 2, m_f = 2\rangle$  and  $|F = 1, m_f = -1\rangle$  spin states of  $^{87}\text{Rb}$ , which is at different hyperfine states of the same species [37]. It demonstrated the possibility of producing long-lived multiple condensate systems, and that the condensate wave function is dramatically affected by the presence of inter-component interactions. While many interesting phenomena have been found in rotating single-component

\* Corresponding author at: Department of Mathematics, National University of Singapore, Singapore 117543, Singapore. Tel.: +65 6516 2765; fax: +65 6774 6756.

*E-mail addresses:* [zhyanzhi@gmail.com](mailto:zhyanzhi@gmail.com) (Y. Zhang), [bao@math.nus.edu.sg](mailto:bao@math.nus.edu.sg) (W. Bao), [hailiang\\_li2002@yahoo.com.cn](mailto:hailiang_li2002@yahoo.com.cn) (H. Li).

*URL:* <http://www.math.nus.edu.sg/~bao/> (W. Bao).

BECs [34,1], a rich variety of static and dynamic phenomena are expected to occur in a system of rotating two-component BEC consisting, for example, of two different hyperfine spin states of atoms [22]. In fact, recent experimental advances in exploration of systems of uniting two or more condensates, e.g. in a magnetic trap in rubidium [37] and subsequently in an optical trap in sodium [42], have spurred great excitement in the atomic physics community and renewed interest in studying the ground states and dynamics of rotating two-component BEC [22,23,36,27].

Theoretical treatment of such systems began in the context of superfluid helium mixtures and spin polarized hydrogen, and has now been extended to BEC in alkalis [23,15,29,39]. With the realization of BEC in experiments, the theoretical predications of multi-component condensates, e.g. density profile, dynamics of interacting BEC [21], motion damping [24] and formation of vortices, can now be compared with experimental data [22,3]. Needless to say that this dramatic progress on the experimental front has stimulated a wave of activity on both theoretical and numerical fronts. In fact, the properties of multi-component BEC, in a rotational frame, at temperatures  $T$  much smaller than the critical condensation temperature  $T_c$  [38,30,31] are usually modelled by the coupled Gross–Pitaevskii equations (CGPEs) for the macroscopic vector wave functions with an angular momentum rotation term and an external driving field [31,30,15]. Note that equations very similar to the CGPEs also appear in nonlinear optics where indices of refraction, which depend on the light intensity, lead to nonlinear terms like those encountered in CGPEs.

There have been extensive mathematical analysis and numerical simulations of the time-independent Gross–Pitaevskii equation (GPE) for ground states [41,5] and time-dependent GPE for dynamics [35,6,5,9] of single-component BEC. For non-rotating two-component BEC, Bao [4] presented a continuous normalized gradient flow (CNGF) with backward Euler finite difference discretization to compute ground state and a time-splitting sine-pseudospectral (TSSP) method to compute dynamics; Chang et al. [11,12] proposed Gauss–Seidel-type methods for studying bound states and segregated nodal domains; Lin and Wei [32, 33] analyzed the existence of ground states and spike solutions; Pérez-García et al. [16] studied the stability and dynamics of quantized vortices; Riboli et al. [40] and Jezek [25] classified different spatial patterns of the ground states; Chui et al. [13] studied quantum phase separation dynamics, the effect of trap displacements and symmetric–asymmetric transition. For rotating two-component BEC, due to the appearance of the angular momentum rotation term and the external driving field, new difficulties are introduced mathematically and numerically. Currently, there has been few analytical results about rotating two-component BEC in the literature. In addition, there is no efficient and accurate numerical method for studying its dynamics. Thus it is of great interest to develop mathematical theories governing the dynamics of rotating two-component BEC and to propose efficient and accurate numerical methods for simulating the CGPEs with an angular momentum rotation term and an external driving field. The aim of this paper is to mathematically find the dynamic laws for the density of each component, condensate width, angular momentum expectation and a stationary state with its center shifted from the trap center, and to present an unconditionally stable numerical method with high-order accuracy for computing the dynamics of rotating two-component BEC. In addition, the numerical method is applied to verify the dynamic laws and to study the dynamics of quantized vortex lattices in rotating two-component BEC. Our extensive numerical results demonstrate that the method is very efficient and accurate.

The paper is organized as follows. In Section 2, we begin with the 3D coupled Gross–Pitaevskii equations (CGPEs) with an angular momentum rotation term and an external driving field, scale them to get dimensionless CGPEs, show how to reduce them to the single GPE in certain limiting regimes and provide their semiclassical scaling, energy asymptotics and geometrical optics in strong repulsive interaction regimes. In Section 3, we propose an efficient and accurate numerical method for discretizing CGPEs and apply it to study the dynamics of quantized vortex lattices. In Section 4, we derive the dynamic laws for the density of each component, angular momentum expectation, condensate width and a stationary state with its center shifted from the trap center, and we also apply our method to numerically verify these laws. Finally, some conclusions are drawn in Section 5.

## 2. Coupled Gross–Pitaevskii equations

At temperatures  $T$  much smaller than the critical temperature  $T_c$  [38,15], in the rotating frame, a two-component BEC with an external driving field can be well described by two self-consistent nonlinear Schrödinger equations (NLSEs), also known as coupled Gross–Pitaevskii equations (CGPEs) [26,17,31,30],

$$i\hbar \frac{\partial \psi_j(\mathbf{x}, t)}{\partial t} = \left[ -\frac{\hbar^2}{2m} \nabla^2 + V_j(\mathbf{x}) - \tilde{\Omega} L_z + \sum_{l=1}^2 U_{jl} |\psi_l|^2 \right] \psi_j - \tilde{\lambda} \hbar \psi_{k_j}, \quad j = 1, 2, \quad (2.1)$$

where  $\psi_j(\mathbf{x}, t)$  denotes the macroscopic wave function of the  $j$ th ( $j = 1, 2$ ) component with  $\mathbf{x} = (x, y, z)^T$  being the Cartesian coordinate vector and  $t$  being time,  $\hbar$  is the Planck constant,  $m$  is the atomic mass (for simplicity, here we assume that the atomic mass of the two components is the same),  $\tilde{\Omega}$  is the angular velocity of the rotating laser beam,  $L_z = -i\hbar(x\partial_y - y\partial_x)$  is the  $z$  component of the angular momentum, and  $\tilde{\lambda}$  is the Rabi frequency describing the strength of the external driving field.  $V_j(\mathbf{x})$  is the external trapping potential acting on the  $j$ th component, and if the harmonic potential is considered, it takes the form

$$V_j(\mathbf{x}) = \frac{m}{2} \left( \omega_{x,j}^2 x^2 + \omega_{y,j}^2 y^2 + \omega_{z,j}^2 z^2 \right), \quad j = 1, 2, \quad (2.2)$$

with  $\omega_{x,j}$ ,  $\omega_{y,j}$  and  $\omega_{z,j}$  the trapping frequencies of the  $j$ th component in  $x$ -,  $y$ - and  $z$ -directions, respectively. The interactions of particles are described by  $U_{jl} = 4\pi \hbar^2 a_{jl}/m$  with  $a_{jl} = a_{lj}$  ( $j, l = 1, 2$ ) being the  $s$ -wave scattering lengths between the  $j$ th and  $l$ th component (positive for repulsive interaction and negative for attractive interaction). The integers  $k_j$  in (2.1) are chosen as

$$k_j = \begin{cases} 2, & j = 1, \\ 1, & j = 2. \end{cases} \quad (2.3)$$

It is necessary to ensure that the wave functions are properly normalized. Especially, we require

$$\int_{\mathbb{R}^3} (|\psi_1(\mathbf{x}, t)|^2 + |\psi_2(\mathbf{x}, t)|^2) d\mathbf{x} = N = N_1^0 + N_2^0, \quad t \geq 0, \quad (2.4)$$

where

$$N_j^0 = \int_{\mathbb{R}^3} |\psi_j(\mathbf{x}, 0)|^2 d\mathbf{x}, \quad (2.5)$$

is the particle number of the  $j$ th ( $j = 1, 2$ ) component at time  $t = 0$  and  $N$  is the total number of particles in the condensate.

### 2.1. Dimensionless CGPEs

Under the normalization (2.4), we introduce the dimensionless variables as follows:  $t \rightarrow t/\omega_{\min}$  with  $\omega_{\min} = \min_{1 \leq j \leq 2} \{\omega_{x,j}, \omega_{y,j}, \omega_{z,j}\}$ ,  $\tilde{\Omega} \rightarrow \omega_{\min} \Omega$ ,  $\tilde{\lambda} \rightarrow \omega_{\min} \lambda$ ,  $\mathbf{x} \rightarrow a_0 \mathbf{x}$  with  $a_0 = \sqrt{\hbar/m\omega_{\min}}$ , and  $\psi_j \rightarrow \psi_j \sqrt{N}/a_0^{3/2}$ , i.e. we choose  $1/\omega_{\min}$  and  $a_0$  as the dimensionless time unit and length unit, respectively. After some computations from (2.1), we obtain the dimensionless CGPEs as

$$i \frac{\partial \psi_j(\mathbf{x}, t)}{\partial t} = \left[ -\frac{1}{2} \nabla^2 + V_j(\mathbf{x}) - \Omega L_z + \sum_{l=1}^2 \beta_{jl} |\psi_l|^2 \right] \psi_j - \lambda \psi_{k_j}, \quad j = 1, 2, \quad (2.6)$$

where the dimensionless interaction parameters are characterized by  $\beta_{jl} = \beta_{lj} = \frac{mU_{jl}N}{\hbar^2 a_0} = \frac{4\pi N a_{jl}}{a_0}$  ( $j, l = 1, 2$ ). The dimensionless angular momentum rotation term becomes

$$L_z = -i(x\partial_y - y\partial_x) = -i\partial_\theta := -i\widehat{L}_z \quad (2.7)$$

with  $(r, \theta)$  the polar coordinate in 2D, and resp.  $(r, \theta, z)$  the cylindrical coordinate in 3D. The dimensionless external potentials are

$$V_j(\mathbf{x}) = \frac{1}{2} (\gamma_{x,j}^2 x^2 + \gamma_{y,j}^2 y^2 + \gamma_{z,j}^2 z^2), \quad j = 1, 2 \quad (2.8)$$

with  $\gamma_{x,j} = \omega_{x,j}/\omega_{\min}$ ,  $\gamma_{y,j} = \omega_{y,j}/\omega_{\min}$  and  $\gamma_{z,j} = \omega_{z,j}/\omega_{\min}$  ( $j = 1, 2$ ).

In a disk-shaped condensate, i.e.

$$\omega_{x,j} \approx \omega_{y,j} \approx \omega_{\min}, \quad \omega_{z,j} \gg \omega_{\min} \iff \gamma_{x,j} \approx \gamma_{y,j} \approx 1, \quad \gamma_{z,j} \gg 1, \quad j = 1, 2,$$

the 3D CGPEs (2.6) can be reduced to 2D CGPEs with  $\mathbf{x} = (x, y)^T$  [35,6,5]. Thus here we consider the following CGPEs in  $d$  dimensions ( $d = 2, 3$ ):

$$i \frac{\partial \psi_j(\mathbf{x}, t)}{\partial t} = \left[ -\frac{1}{2} \nabla^2 + V_j(\mathbf{x}) - \Omega L_z + \sum_{l=1}^2 \beta_{jl} |\psi_l|^2 \right] \psi_j - \lambda \psi_{k_j}, \quad t \geq 0, \quad (2.9)$$

$$\psi_j(\mathbf{x}, 0) = \psi_j^0(\mathbf{x}), \quad \mathbf{x} \in \mathbb{R}^d, \quad (2.10)$$

where the initial data are normalized as

$$\|\psi_1^0\|^2 + \|\psi_2^0\|^2 := \int_{\mathbb{R}^d} (|\psi_1^0(\mathbf{x})|^2 + |\psi_2^0(\mathbf{x})|^2) d\mathbf{x} = \frac{N_1^0}{N} + \frac{N_2^0}{N} = 1,$$

and the external potentials are given as

$$V_j(\mathbf{x}) = \begin{cases} \frac{1}{2} (\gamma_{x,j}^2 x^2 + \gamma_{y,j}^2 y^2), & d = 2, \\ \frac{1}{2} (\gamma_{x,j}^2 x^2 + \gamma_{y,j}^2 y^2 + \gamma_{z,j}^2 z^2), & d = 3, \end{cases} \quad j = 1, 2. \quad (2.11)$$

The dimensionless CGPEs (2.9) conserve the total density:

$$N(t) = N_1(t) + N_2(t) \equiv \|\psi_1^0\|^2 + \|\psi_2^0\|^2 = 1, \quad t \geq 0 \quad (2.12)$$

with

$$N_j(t) = \|\psi_j(\cdot, t)\|^2 := \int_{\mathbb{R}^d} |\psi_j(\mathbf{x}, t)|^2 d\mathbf{x}, \quad t \geq 0, j = 1, 2, \quad (2.13)$$

and the energy

$$\begin{aligned} E(\psi_1, \psi_2) &= \int_{\mathbb{R}^d} \left[ \sum_{j=1}^2 \left( \frac{1}{2} |\nabla \psi_j|^2 + V_j(\mathbf{x}) |\psi_j|^2 - \Omega \operatorname{Re}(\psi_j^* L_z \psi_j) + \sum_{l=1}^2 \frac{\beta_{jl}}{2} |\psi_j|^2 |\psi_l|^2 \right) - 2\lambda \operatorname{Re}(\psi_1^* \psi_2) \right] d\mathbf{x} \\ &\equiv E(\psi_1^0, \psi_2^0), \quad t \geq 0 \end{aligned} \quad (2.14)$$

with  $f^*$  and  $\operatorname{Re}(f)$  denoting the conjugate and real part of a function  $f$ , respectively. In addition, if there is no external driving field in (2.9), i.e.  $\lambda = 0$ , the density of each component is also conserved, i.e.

$$N_j(t) = \int_{\mathbb{R}^d} |\psi_j(\mathbf{x}, t)|^2 d\mathbf{x} \equiv \|\psi_j^0\|^2 = \frac{N_j^0}{N}, \quad t \geq 0, j = 1, 2. \quad (2.15)$$

## 2.2. Reduction to single GPE

If there is no external driving field in (2.9), i.e.  $\lambda = 0$ , and the initial particle numbers of the two components  $N_1^0$  and  $N_2^0$  (w.l.o.g., assuming that  $N_1^0 \geq N_2^0$ ) in (2.4) satisfy  $N_1^0 \gg N_2^0$ , i.e.  $N_1^0 = O(N)$  and  $N_2^0 = o(N)$ , when  $N \gg 1$ , we have

$$N_2(t) = \int_{\mathbb{R}^d} |\psi_2(\mathbf{x}, t)|^2 d\mathbf{x} \equiv \frac{N_2^0}{N} := \varepsilon \ll 1, \quad (2.16)$$

$$N_1(t) = \int_{\mathbb{R}^d} |\psi_1(\mathbf{x}, t)|^2 d\mathbf{x} \equiv \frac{N_1^0}{N} := 1 - \varepsilon \approx 1, \quad t \geq 0. \quad (2.17)$$

These immediately imply that the effect of the second component is insignificant and the original two-component system is mainly dominated by the first component. Formally, we can drop the second component from the two-component BEC and get a single-component BEC, and in this case the CGPEs (2.9) are reduced to

$$i \frac{\partial \psi(\mathbf{x}, t)}{\partial t} = \left[ -\frac{1}{2} \nabla^2 + V(\mathbf{x}) + \beta |\psi|^2 - \Omega L_z \right] \psi, \quad t \geq 0 \quad (2.18)$$

by setting  $\psi(\mathbf{x}, t) = \sqrt{N/N_1^0} \psi_1(\mathbf{x}, t)$ ,  $V(\mathbf{x}) = V_1(\mathbf{x})$  and  $\beta = N_1^0 \beta_{11}/N \approx \beta_{11}$ . The GPE (2.18) conserves the normalization of the wave function

$$\|\psi(\cdot, t)\|^2 \equiv \int_{\mathbb{R}^d} |\psi(\mathbf{x}, t)|^2 d\mathbf{x} = \int_{\mathbb{R}^d} \frac{N}{N_1^0} |\psi_1(\mathbf{x}, 0)|^2 d\mathbf{x} = \frac{N}{N_1^0} \frac{N_1^0}{N} = 1, \quad t \geq 0, \quad (2.19)$$

and the energy

$$E_s(\psi) = \int_{\mathbb{R}^d} \left[ \frac{1}{2} |\nabla \psi|^2 + V(\mathbf{x}) |\psi|^2 - \Omega \operatorname{Re}(\psi^* L_z \psi) + \frac{\beta}{2} |\psi|^4 \right] d\mathbf{x}, \quad t \geq 0. \quad (2.20)$$

In addition, by setting  $\psi_1(\mathbf{x}, t) = \sqrt{N_1^0/N} \psi(\mathbf{x}, t)$  and  $\psi_2(\mathbf{x}, t) = \sqrt{N_2^0/N} \phi(\mathbf{x}, t)$  in the energy of the two-component BEC (2.14) with  $\lambda = 0$ , we obtain

$$\begin{aligned} E(\psi_1, \psi_2) &= \frac{N_1^0}{N} E_s(\psi) + \frac{N_2^0}{N} E_r(\psi, \phi) = (1 - \varepsilon) E_s(\psi) + \varepsilon E_r(\psi, \phi) \\ &= E_s(\psi) + \varepsilon [-E_s(\psi) + E_r(\psi, \phi)], \end{aligned} \quad (2.21)$$

where

$$E_r(\psi, \phi) = \int_{\mathbb{R}^d} \left[ \frac{1}{2} |\nabla \phi|^2 + V_2(\mathbf{x}) |\phi|^2 - \Omega \operatorname{Re}(\phi^* L_z \phi) + \beta_{21} \frac{N_1^0}{N} |\psi|^2 |\phi|^2 + \frac{\beta_{22}}{2} \frac{N_2^0}{N} |\phi|^4 \right] d\mathbf{x}.$$

This formally implies that the relative error between the energy of the two-component BEC (2.14) and that of the single-component BEC (2.20) converges to 0 linearly when  $\varepsilon = \frac{N_0^0}{N}$  goes to 0, i.e.

$$\frac{|E(\psi_1, \psi_2) - E_s(\psi)|}{E_s(\psi)} = \varepsilon \left( 1 - \frac{E_r(\psi, \phi)}{E_s(\psi)} \right) = O(\varepsilon), \quad \text{when } 0 < \varepsilon \ll 1. \quad (2.22)$$

### 2.3. Semiclassical scaling and geometrical optics

Let  $\beta_{\max} = \max\{\beta_{11}, \beta_{12}, \beta_{22}\}$ . If  $\beta_{\max} \gg 1$ , i.e. in the strong repulsive interaction regime or there are many particles in the condensate, under the normalization (2.12), the semiclassical scaling for the CGPEs (2.9) is also very useful in practice by choosing

$$\mathbf{x} = \varepsilon^{-1/2} \mathbf{x}, \quad \psi_j^\varepsilon = \varepsilon^{d/4} \psi_j, \quad \varepsilon = \beta_{\max}^{-2/(d+2)}. \quad (2.23)$$

Substituting (2.23) into (2.9), we get the CGPEs in the semiclassical scaling under the normalization (2.12) with  $\psi_j = \psi_j^\varepsilon$  ( $j = 1, 2$ ):

$$i\varepsilon \frac{\partial \psi_j^\varepsilon(\mathbf{x}, t)}{\partial t} = \left[ -\frac{\varepsilon^2}{2} \nabla^2 + V_j(\mathbf{x}) - \varepsilon \Omega L_z + \sum_{l=1}^2 \alpha_{jl} |\psi_l^\varepsilon|^2 \right] \psi_j^\varepsilon - \varepsilon \lambda \psi_{k_j}^\varepsilon, \quad j = 1, 2, \quad (2.24)$$

where  $\alpha_{jl} = \beta_{jl}/\beta_{\max} = O(1)$  (or  $o(1)$ ). In this case, the energy functional  $E^\varepsilon(\psi_1^\varepsilon, \psi_2^\varepsilon)$  is defined as

$$\begin{aligned} E^\varepsilon(\psi_1^\varepsilon, \psi_2^\varepsilon) = \int_{\mathbb{R}^d} \left[ \sum_{j=1}^2 \left( \frac{\varepsilon^2}{2} |\nabla \psi_j^\varepsilon|^2 + V_j(\mathbf{x}) |\psi_j^\varepsilon|^2 - \varepsilon \Omega \operatorname{Re} \left( (\psi_j^\varepsilon)^* L_z \psi_j^\varepsilon \right) \right. \right. \\ \left. \left. + \sum_{l=1}^2 \frac{\alpha_{jl}}{2} |\psi_j^\varepsilon|^2 |\psi_l^\varepsilon|^2 \right) - 2\varepsilon \lambda \operatorname{Re} \left( (\psi_1^\varepsilon)^* \psi_2^\varepsilon \right) \right] d\mathbf{x} = O(1), \quad t \geq 0, \end{aligned} \quad (2.25)$$

by assuming that  $\psi_j^\varepsilon$  is  $\varepsilon$ -oscillatory (see (2.27)) and ‘sufficiently’ integrable such that all terms have  $O(1)$ -integral. Then the leading asymptotics of the energy functional  $E(\psi_1, \psi_2)$  in (2.14) can be given by

$$E(\psi_1, \psi_2) = \varepsilon^{-1} E^\varepsilon(\psi_1^\varepsilon, \psi_2^\varepsilon) = O(\varepsilon^{-1}) = O\left(\beta_{\max}^{2/(d+2)}\right). \quad (2.26)$$

If  $\lambda = 0$  and  $0 < \varepsilon \ll 1$  in (2.24), we can set, i.e. the WKB ansatz [19]

$$\psi_j^\varepsilon(\mathbf{x}, t) = \sqrt{\rho_j^\varepsilon(\mathbf{x}, t)} \exp\left(\frac{i}{\varepsilon} S_j^\varepsilon(\mathbf{x}, t)\right), \quad j = 1, 2, \quad (2.27)$$

where  $\rho_j^\varepsilon = |\psi_j^\varepsilon|^2$  and  $S_j^\varepsilon = \varepsilon \arg(\psi_j^\varepsilon)$  are the position density and phase of the wave function  $\psi_j^\varepsilon$  of  $j$ th component ( $j = 1, 2$ ), respectively. Inserting (2.27) into (2.24) and collecting the real and imaginary parts, we get the coupled transport equations for the densities  $\rho_j^\varepsilon$  and the Hamilton–Jacobi equations for the phases  $S_j^\varepsilon$  ( $j = 1, 2$ ):

$$\partial_t \rho_j^\varepsilon + \operatorname{div} \left( \rho_j^\varepsilon \nabla S_j^\varepsilon \right) + \Omega \widehat{L}_z \rho_j^\varepsilon = 0, \quad (2.28)$$

$$\partial_t S_j^\varepsilon + \frac{1}{2} |\nabla S_j^\varepsilon|^2 + V_j(\mathbf{x}) + \sum_{l=1}^2 \alpha_{jl} \rho_l^\varepsilon = \frac{\varepsilon^2}{2\sqrt{\rho_j^\varepsilon}} \nabla^2 \sqrt{\rho_j^\varepsilon}, \quad j = 1, 2. \quad (2.29)$$

Furthermore, by defining the current densities

$$\mathbf{J}_j^\varepsilon(\mathbf{x}, t) = \rho_j^\varepsilon \nabla S_j^\varepsilon = \varepsilon \operatorname{Im} \left[ \left( \psi_j^\varepsilon \right)^* \nabla \psi_j^\varepsilon \right], \quad j = 1, 2, \quad (2.30)$$

where  $\operatorname{Im}(f)$  is the imaginary part of a function  $f$ , we can rewrite (2.28)–(2.29) as a coupled Euler system with third-order dispersion terms

$$\partial_t \rho_j^\varepsilon + \operatorname{div} \mathbf{J}_j^\varepsilon + \Omega \widehat{L}_z \rho_j^\varepsilon = 0, \quad j = 1, 2, \quad (2.31)$$

$$\partial_t \mathbf{J}_j^\varepsilon + \operatorname{div} \left( \frac{\mathbf{J}_j^\varepsilon \otimes \mathbf{J}_j^\varepsilon}{\rho_j^\varepsilon} \right) + \rho_j^\varepsilon \nabla V_j(\mathbf{x}) + \nabla P_j(\rho_1^\varepsilon, \rho_2^\varepsilon) + \Omega (\widehat{L}_z + \mathbf{G}) \mathbf{J}_j^\varepsilon = \frac{\varepsilon^2}{4} \nabla \left( \rho_j^\varepsilon \nabla^2 \ln \rho_j^\varepsilon \right), \quad (2.32)$$

where the symplectic matrix  $\mathbf{G}$  is defined as

$$\mathbf{G} = \begin{pmatrix} 0 & 1 \\ -1 & 0 \end{pmatrix}, \quad \text{for } d = 2, \quad \mathbf{G} = \begin{pmatrix} 0 & 1 & 0 \\ -1 & 0 & 0 \\ 0 & 0 & 0 \end{pmatrix}, \quad \text{for } d = 3, \quad (2.33)$$

and the pressures  $P_j$  are defined as

$$P_j(\rho_1^\varepsilon, \rho_2^\varepsilon) = \frac{1}{2} \sum_{l=1}^2 \alpha_{jl} \rho_j^\varepsilon \rho_l^\varepsilon, \quad j = 1, 2.$$

By formally passing to the limit  $\varepsilon \rightarrow 0^+$  in (2.28)–(2.29), we get

$$\partial_t \rho_j^0 + \operatorname{div} \left( \rho_j^0 \nabla S_j^0 \right) + \Omega \widehat{L}_z \rho_j^0 = 0, \quad (2.34)$$

$$\partial_t S_j^0 + \frac{1}{2} |\nabla S_j^0|^2 + V_j(\mathbf{x}) + \sum_{l=1}^2 \alpha_{jl} \rho_l^0 = 0, \quad j = 1, 2, \quad (2.35)$$

with  $\rho_j^0 = \lim_{\varepsilon \rightarrow 0^+} \rho_j^\varepsilon$  and  $S_j^0 = \lim_{\varepsilon \rightarrow 0^+} S_j^\varepsilon$ . Similarly, letting  $\varepsilon \rightarrow 0^+$  in (2.31)–(2.32), formally we get an Euler system coupling through the pressures

$$\partial_t \rho_j^0 + \operatorname{div} \mathbf{J}_j^0 + \Omega \widehat{L}_z \rho_j^0 = 0, \quad j = 1, 2, \quad (2.36)$$

$$\partial_t \mathbf{J}_j^0 + \operatorname{div} \left( \frac{\mathbf{J}_j^0 \otimes \mathbf{J}_j^0}{\rho_j^0} \right) + \rho_j^0 \nabla V_j(\mathbf{x}) + \nabla P_j(\rho_1^0, \rho_2^0) + \Omega (\widehat{L}_z + \mathbf{G}) \mathbf{J}_j^0 = 0, \quad (2.37)$$

where  $\mathbf{J}_j^0(\mathbf{x}, t) = \rho_j^0 \nabla S_j^0$  ( $j = 1, 2$ ). The system (2.36)–(2.37) is a coupled isotropic Euler system with quadratic pressure–density constitutive relations in the rotational frame. The formal asymptotics is supposed to hold up to caustic onset time [19,20].

**Remark 2.1.** When  $\lambda \neq 0$  in (2.24), the WKB analysis for studying the semiclassical limit of the nonlinear Schrödinger equation [19] is no longer valid for (2.24). Alternatively, one may need to use the Wigner transform [20] to study the semiclassical limit of (2.24) when  $\lambda \neq 0$ .

### 3. Numerical methods

In this section, we present an efficient and accurate numerical method to solve the CGPEs (2.9)–(2.10) for the dynamics of rotating two-component BEC. The key ideas are to apply a time-splitting technique for decoupling the nonlinearity and to adopt the polar coordinate in 2D, and resp. cylindrical coordinate in 3D, such that the angular momentum rotation term becomes a term with constant coefficients. Due to the trapping potentials  $V_1(\mathbf{x})$  and  $V_2(\mathbf{x})$  given by (2.11), the solution  $(\psi_1, \psi_2)$  of (2.9)–(2.10) decays to zero exponentially fast when  $|\mathbf{x}| \rightarrow \infty$ . Thus in practical computation, we truncate the problem (2.9)–(2.10) into a bounded computational domain  $\Omega_{\mathbf{x}}$  with homogeneous Dirichlet boundary conditions:

$$i \frac{\partial \psi_j}{\partial t} = \left[ -\frac{1}{2} \nabla^2 + V_j(\mathbf{x}) - \Omega L_z + \sum_{l=1}^2 \beta_{jl} |\psi_l|^2 \right] \psi_j - \lambda \psi_{k_j}, \quad \mathbf{x} \in \Omega_{\mathbf{x}}, t \geq 0, \quad (3.1)$$

$$\psi_j(\mathbf{x}, t) = 0, \quad \mathbf{x} \in \Gamma = \partial \Omega_{\mathbf{x}}, \quad t \geq 0, \quad (3.2)$$

$$\psi_j(\mathbf{x}, 0) = \psi_j^0(\mathbf{x}), \quad \mathbf{x} \in \overline{\Omega_{\mathbf{x}}}, \quad \text{with } \int_{\Omega_{\mathbf{x}}} \left( |\psi_1^0(\mathbf{x})|^2 + |\psi_2^0(\mathbf{x})|^2 \right) d\mathbf{x} = 1. \quad (3.3)$$

In practical computation, we use sufficiently large domain so as to make sure the homogeneous Dirichlet boundary condition (3.2) does not introduce aliasing error. Usually, the radius of the bounded computational domain depends on the problem. In general, it should be larger than the “Thomas–Fermi radius”. Of course, the use of more sophisticated radiation boundary conditions is an interesting topic that remains to be examined in the future.

#### 3.1. Time-splitting

We choose a time step  $\Delta t > 0$ . For  $n = 0, 1, \dots$ , from time  $t = t_n = n\Delta t$  to  $t = t_{n+1} = t_n + \Delta t$ , the CGPEs (3.1) are solved in three splitting steps [4,6]. One first solves

$$i \frac{\partial \psi_j}{\partial t} = -\frac{1}{2} \nabla^2 \psi_j - \Omega L_z \psi_j, \quad j = 1, 2 \quad (3.4)$$

for the time step of length  $\Delta t$ , followed by solving

$$i \frac{\partial \psi_j}{\partial t} = V_j(\mathbf{x}) \psi_j + \sum_{l=1}^2 \beta_{jl} |\psi_l|^2 \psi_j, \quad j = 1, 2 \quad (3.5)$$

for the same time step, and then by solving

$$i \frac{\partial \psi_j}{\partial t} = -\lambda \psi_{k_j}, \quad j = 1, 2 \quad (3.6)$$

again for the same time step. For time  $t \in [t_n, t_{n+1}]$ , the ODE system (3.5) leaves  $|\psi_1(\mathbf{x}, t)|$  and  $|\psi_2(\mathbf{x}, t)|$  invariant in  $t$  [4,6], and thus it can be integrated *exactly* to obtain [4,5], for  $j = 1, 2$  and  $t \in [t_n, t_{n+1}]$

$$\psi_j(\mathbf{x}, t) = \psi_j(\mathbf{x}, t_n) \exp \left[ -i \left( V_j(\mathbf{x}) + \sum_{l=1}^2 \beta_{jl} |\psi_l(\mathbf{x}, t_n)|^2 \right) (t - t_n) \right]. \quad (3.7)$$

For the ODE system (3.6), we can rewrite it as

$$i \frac{\partial \Psi}{\partial t} = -\lambda A \Psi, \quad \text{with } A = \begin{pmatrix} 0 & 1 \\ 1 & 0 \end{pmatrix} \text{ and } \Psi = \begin{pmatrix} \psi_1 \\ \psi_2 \end{pmatrix}. \quad (3.8)$$

Since  $A$  is a real and symmetric matrix, it can be diagonalized and integrated *exactly*, and then we obtain [4], for  $t \in [t_n, t_{n+1}]$

$$\Psi(\mathbf{x}, t) = e^{i\lambda A(t-t_n)} \Psi(\mathbf{x}, t_n) = \begin{pmatrix} \cos(\lambda(t-t_n)) & i \sin(\lambda(t-t_n)) \\ i \sin(\lambda(t-t_n)) & \cos(\lambda(t-t_n)) \end{pmatrix} \Psi(\mathbf{x}, t_n). \quad (3.9)$$

The Eqs. (3.1) are now decoupled and thus we need only show how to discretize the following single GPE in a rotational frame:

$$i \frac{\partial \psi}{\partial t} = -\frac{1}{2} \nabla^2 \psi - \Omega L_z \psi, \quad \mathbf{x} \in \Omega_{\mathbf{x}}, t_n \leq t \leq t_{n+1}. \quad (3.10)$$

Various algorithms were introduced in the literature for discretizing the GPE (3.10) [5,44,7]. For the convenience of the reader, here we review a method which discretizes the Eq. (3.10) in the  $\theta$ -direction by the Fourier-pseudospectral method, in the  $r$ -direction by the fourth-order finite difference method, in the  $z$ -direction by the sine-pseudospectral method and in time by the Crank–Nicolson (C–N) scheme [5]. In order to do so, we choose the bounded computational domain  $\Omega_{\mathbf{x}} = \{(x, y), r = \sqrt{x^2 + y^2} < R\}$  in 2D, and resp.  $\Omega_{\mathbf{x}} = \{(x, y, z), r = \sqrt{x^2 + y^2} < R, a < z < b\}$  in 3D with  $R$ ,  $|a|$ , and  $b$  sufficiently larger than the Thomas–Fermi radii.

### 3.2. Discretization in 2D

When  $d = 2$ , we use the polar coordinate  $(r, \theta)$  and assume that

$$\psi(r, \theta, t) = \sum_{l=-L/2}^{L/2-1} \widehat{\psi}_l(r, t) e^{il\theta}, \quad (3.11)$$

where  $L$  is an even positive integer and  $\widehat{\psi}_l(r, t)$  is the Fourier coefficient for the  $l$ th mode. Plugging (3.11) into (3.10) and noticing the orthogonality of the Fourier functions, we obtain, for  $-\frac{L}{2} \leq l \leq \frac{L}{2} - 1$  and  $0 < r < R$ :

$$i \frac{\partial \widehat{\psi}_l(r, t)}{\partial t} = -\frac{1}{2r} \frac{\partial}{\partial r} \left( r \frac{\partial \widehat{\psi}_l(r, t)}{\partial r} \right) + \left( \frac{l^2}{2r^2} - l\Omega \right) \widehat{\psi}_l(r, t), \quad (3.12)$$

$$\widehat{\psi}_l(R, t) = 0, \quad (\text{for all } l), \quad \widehat{\psi}_l(0, t) = 0, \quad (\text{for } l \neq 0). \quad (3.13)$$

In order to discretize (3.12)–(3.13) in space by the finite difference method, we choose an integer  $M > 0$ , a mesh size  $\Delta r = 2R/(2M + 1)$  and grid points  $r_m = (m - 1/2)\Delta r$  for  $1 \leq m \leq M + 1$ . Let  $\widehat{\psi}_{l,m}(t)$  be the approximation of  $\widehat{\psi}_l(r_m, t)$ . Then a fourth-order finite difference discretization for (3.12)–(3.13) with  $t \in [t_n, t_{n+1}]$  reads [5,28]

$$i \frac{d\widehat{\psi}_{l,m}(t)}{dt} = \left( \frac{l^2}{2r_m^2} - l\Omega \right) \widehat{\psi}_{l,m}(t) - \frac{-\widehat{\psi}_{l,m+2}(t) + 16\widehat{\psi}_{l,m+1}(t) - 30\widehat{\psi}_{l,m}(t) + 16\widehat{\psi}_{l,m-1}(t) - \widehat{\psi}_{l,m-2}(t)}{24(\Delta r)^2} \\ - \frac{-\widehat{\psi}_{l,m+2}(t) + 8\widehat{\psi}_{l,m+1}(t) - 8\widehat{\psi}_{l,m-1}(t) + \widehat{\psi}_{l,m-2}(t)}{24r_m \Delta r}, \quad 1 \leq m \leq M, \quad (3.14)$$

$$i \frac{d\widehat{\psi}_{l,M+1}(t)}{dt} = \left( \frac{l^2}{2r_{M+1}^2} - l\Omega \right) \widehat{\psi}_{l,M+1}(t) - \frac{11\widehat{\psi}_{l,M+2}(t) - 20\widehat{\psi}_{l,M+1}(t) + 6\widehat{\psi}_{l,M}(t) + 4\widehat{\psi}_{l,M-1}(t) - \widehat{\psi}_{l,M-2}(t)}{24(\Delta r)^2} - \frac{3\widehat{\psi}_{l,M+2}(t) + 10\widehat{\psi}_{l,M+1}(t) - 18\widehat{\psi}_{l,M}(t) + 6\widehat{\psi}_{l,M-1}(t) - \widehat{\psi}_{l,M-2}(t)}{24r_{M+1}\Delta r}, \quad (3.15)$$

$$\widehat{\psi}_{l,-1}(t) = (-1)^l \widehat{\psi}_{l,2}(t), \quad \widehat{\psi}_{l,0}(t) = (-1)^l \widehat{\psi}_{l,1}(t), \quad \widehat{\psi}_{l,M+1}(t) = 0. \quad (3.16)$$

Finally, the ODE system (3.14)–(3.16) is discretized by the standard C–N scheme in time. Although an implicit time discretization is applied for (3.14)–(3.16), the 1D nature of the problem makes the coefficient matrix for the linear system pentadiagonal, which can be solved very efficiently, i.e. via  $O(M)$  arithmetic operations.

In practice, we always use the second-order Strang splitting [43]; i.e. from time  $t = t_n$  to  $t = t_{n+1}$  (i) evolve (3.5) for half time step  $\Delta t/2$  with the initial data given at  $t = t_n$ ; (ii) evolve (3.6) for half time step  $\Delta t/2$  with the new data; (iii) evolve (3.4) for time step  $\Delta t$  with the new data obtained in (ii); (iv) evolve (3.6) for half time step  $\Delta t/2$  with the new data obtained in (iii), and (v) evolve (3.5) for half time step  $\Delta t/2$  with the newer data.

For the discretization considered here, the total memory requirement is  $O(ML)$  and the total computational cost per time step is  $O(ML \ln L)$ . The method is time reversible and time transverse invariant when the original CGPEs (2.9) does. Furthermore, following the similar proofs in [4,6,5], the total density can be shown to be conserved in the discretized level.

**Remark 3.1.** When  $\lambda = 0$  in (3.1), in the above second-order Strang splitting for the problem, the step (ii) and (iv) can be removed, and then the method will consist of three steps. In this case, the density of each component is also conserved in the discretized level. In addition, a second-order finite difference discretization for (3.12)–(3.13) was proposed in [5].

### 3.3. Discretization in 3D

When  $d = 3$ , we use the cylindrical coordinate  $(r, \theta, z)$  and assume that

$$\psi(r, \theta, z, t) = \sum_{l=-L/2}^{L/2-1} \sum_{k=1}^{K-1} \widehat{\psi}_{l,k}(r, t) e^{il\theta} \sin(\mu_k(z-a)), \quad (3.17)$$

where  $L$  and  $K$  are two even positive integers,  $\mu_k = \frac{\pi k}{b-a}$  ( $k = 1, \dots, K-1$ ) and  $\widehat{\psi}_{l,k}(r, t)$  is the Fourier-sine coefficient for the  $(l, k)$ th mode. Plugging (3.17) into (3.10) with  $d = 3$ , noticing the orthogonality of the Fourier-sine modes, we obtain, for  $-\frac{L}{2} \leq l \leq \frac{L}{2} - 1$ ,  $1 \leq k \leq K-1$  and  $0 < r < R$ , that

$$i \frac{\partial \widehat{\psi}_{l,k}(r, t)}{\partial t} = -\frac{1}{2r} \frac{\partial}{\partial r} \left( r \frac{\partial \widehat{\psi}_{l,k}(r, t)}{\partial r} \right) + \left( \frac{l^2}{2r^2} + \frac{\mu_k^2}{2} - l\Omega \right) \widehat{\psi}_{l,k}(r, t), \quad (3.18)$$

with essential boundary conditions

$$\widehat{\psi}_{l,k}(R, t) = 0 \quad (\text{for all } l), \quad \widehat{\psi}_{l,k}(0, t) = 0 \quad (\text{for } l \neq 0). \quad (3.19)$$

The discretization of (3.18)–(3.19) is similar as that for (3.12)–(3.13) and thus omitted here.

For the algorithm in 3D, the total memory requirement is  $O(MLK)$  and the total computational cost per time step is  $O(MLK \ln(LK))$ .

### 3.4. Dynamics of vortex lattices

To demonstrate the efficiency and accuracy of our method, we apply it to study the dynamics of quantized vortex lattices in rotating two-component BEC. In our computations, we take  $d = 2$  and  $R = 12$  for  $\Omega_x$  in (3.1)–(3.3), and choose mesh sizes  $\Delta r = 0.005$ ,  $\Delta \theta = \pi/128$  and time step  $\Delta t = 0.0001$ .

The parameters are chosen as  $\Omega = 0.9$ ,  $\beta_{11} = \beta_{22} = 200$  and  $\beta_{12} = 160$  in (2.9), which corresponds to an experimental setup with the following parameters:  $\hbar = 1.054 \times 10^{-34}$  [J s],  $m = 1.443 \times 10^{-25}$  [kg],  $\omega_{\min} = 2\pi \times 200$  [Hz],  $a_{11} = a_{22} = 5.5 \times 10^{-9}$  [m],  $a_{12} = 4.4 \times 10^{-9}$  [m],  $\tilde{\Omega} = 2\pi \times 180$  [Hz] and  $N_1^0 = N_2^0 = 1100$  [22,25,26]. The initial data in (2.10) is taken as the stationary square vortex lattices [26], which are computed by using the above parameters as well as  $\lambda = 0$  and  $\gamma_{x,j} = \gamma_{y,j} = 1$  ( $j = 1, 2$ ) in (2.9). Figs. 1 and 2 depict the contour plots of the wave functions  $|\psi_1|^2$  and  $|\psi_2|^2$  at different times for two cases: (i) adding an external driving field, i.e. at  $t = 0$ , changing  $\lambda$  in (2.9) from 0 to 1, and (ii) changing the trapping frequencies, i.e. at  $t = 0$ , setting  $\gamma_{x,1} = \gamma_{y,1} = 0.9$  and  $\gamma_{x,2} = \gamma_{y,2} = 1.1$ , respectively.

From Figs. 1 and 2, we can see that initially there are two square lattices with about 16 and 21 quantized vortices in the first and second components, respectively (cf. Figs. 1 and 2 leftmost column). When we add an external driving field at  $t = 0$ , the two vortex lattices rotate due to the angular momentum term and shift their condensate shapes almost periodically due to the external driving field (cf. Fig. 1). On the other hand, if we change the trapping frequencies at time  $t = 0$ , the two vortex lattices rotate again due

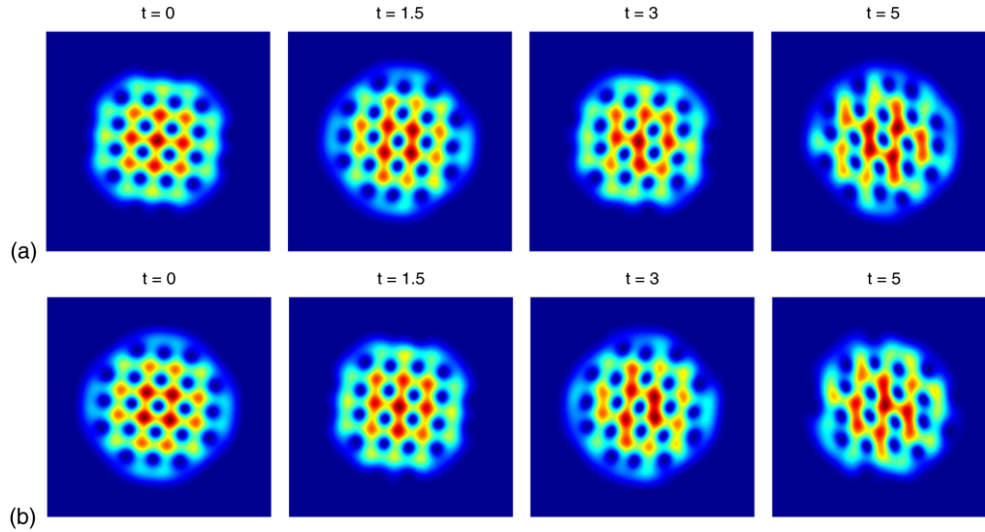


Fig. 1. Contour plots of the wave functions  $|\psi_1|^2$  (top row (a)) and  $|\psi_2|^2$  (bottom row (b)) at different times for case (i).

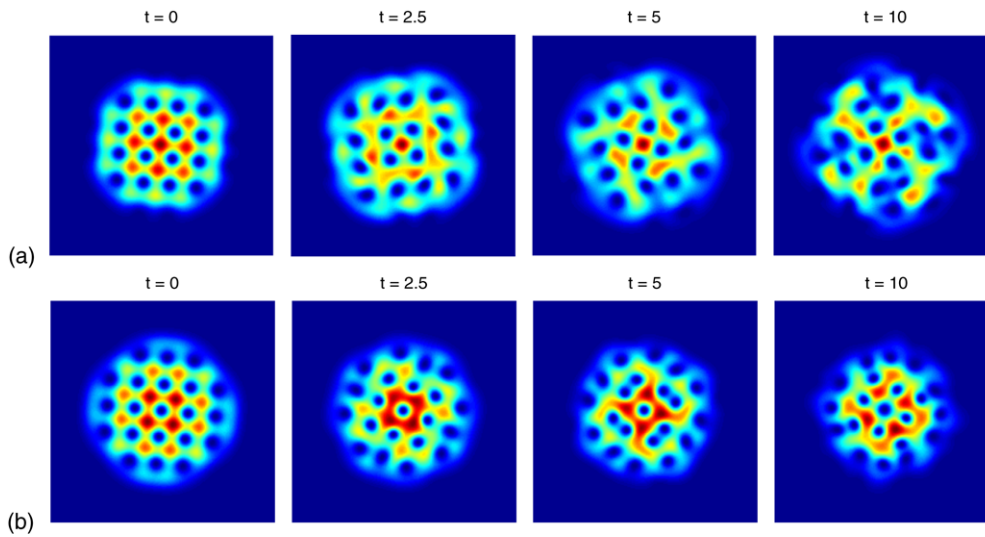


Fig. 2. Contour plots of the wave functions  $|\psi_1|^2$  (top row (a)) and  $|\psi_2|^2$  (bottom row (b)) at different times for case (ii).

to the angular momentum term but the condensate shape of each component keeps almost unchanged and the number of vortices in each lattice does not change during the dynamics (cf. Fig. 2). Of course, the lattice patterns are changed due to the inter-component interactions (cf. Figs. 1 and 2). The numerical results demonstrate the efficiency and high-resolution of our numerical method.

#### 4. Dynamics of rotating two-component BEC

In this section, we study the dynamics of rotating two-component BEC. From an analytical perspective, we prove the conservation of the angular momentum expectation in symmetric traps, derive second-order ordinary differential equations (ODEs) for time evolution of the density of each component and condensate widths, and present some dynamic laws for a stationary state with its center shifted from the trap center in rotating two-component BEC. In addition, we also apply our numerical method to verify these analytical results numerically.

##### 4.1. Dynamics of the density of each component

As we know, when  $\lambda = 0$  in (2.9), the density of each component is conserved as specified in (2.15). While when  $\lambda \neq 0$ , we have the following lemmas for the dynamics of the density of each component:

**Lemma 4.1.** *Suppose  $(\psi_1(\mathbf{x}, t), \psi_2(\mathbf{x}, t))$  is the solution of the CGPEs (2.9)–(2.10); then we have, for  $j = 1, 2$*

$$N_j''(t) = -2\lambda^2 [2N_j(t) - 1] + F_j(t), \quad t \geq 0, \tag{4.1}$$

with initial conditions

$$N_j(0) = N_j^{(0)} = \int_{\mathbb{R}^d} |\psi_j^0(\mathbf{x})|^2 d\mathbf{x} = \frac{N_j^0}{N}, \quad (4.2)$$

$$N_j'(0) = N_j^{(1)} = 2\lambda \int_{\mathbb{R}^d} \text{Im} \left[ \psi_j^0(\mathbf{x}) \left( \psi_{k_j}^0(\mathbf{x}) \right)^* \right] d\mathbf{x}; \quad (4.3)$$

where for  $t \geq 0$ ,

$$F_j(t) = \lambda \int_{\mathbb{R}^d} \left( \psi_j^* \psi_{k_j} + \psi_j \psi_{k_j}^* \right) \left[ V_{k_j}(\mathbf{x}) - V_j(\mathbf{x}) - (\beta_{jj} - \beta_{k_j k_j}) |\psi_j|^2 + (\beta_{k_j k_j} - \beta_{j k_j}) |\psi_{k_j}|^2 \right] d\mathbf{x}, \quad t \geq 0.$$

**Proof.** Differentiating (2.13) with respect to  $t$ , noting (2.9) and integrating by parts, we obtain for  $j = 1, 2$

$$\begin{aligned} N_j'(t) &= \frac{d}{dt} \|\psi_j(\cdot, t)\|^2 = \frac{d}{dt} \int_{\mathbb{R}^d} |\psi_j(\mathbf{x}, t)|^2 d\mathbf{x} = \int_{\mathbb{R}^d} \left( \psi_j \partial_t \psi_j^* + \psi_j^* \partial_t \psi_j \right) d\mathbf{x} \\ &= i \int_{\mathbb{R}^d} \left[ \psi_j \left( -\frac{1}{2} \nabla^2 \psi_j^* + V_j(\mathbf{x}) \psi_j^* - \Omega L_z^* \psi_j^* + \psi_j^* \sum_{l=1}^2 \beta_{jl} |\psi_l|^2 - \lambda \psi_{k_j}^* \right) \right. \\ &\quad \left. - \psi_j^* \left( -\frac{1}{2} \nabla^2 \psi_j + V_j(\mathbf{x}) \psi_j - \Omega L_z \psi_j + \psi_j \sum_{l=1}^2 \beta_{jl} |\psi_l|^2 - \lambda \psi_{k_j} \right) \right] d\mathbf{x} \\ &= i \int_{\mathbb{R}^d} \left[ \left( \frac{1}{2} |\nabla \psi_j|^2 + V_j(\mathbf{x}) |\psi_j|^2 - \psi_j^* \Omega L_z \psi_j + |\psi_j|^2 \sum_{l=1}^2 \beta_{jl} |\psi_l|^2 \right) \right. \\ &\quad \left. - \left( \frac{1}{2} |\nabla \psi_j|^2 + V_j(\mathbf{x}) |\psi_j|^2 - \psi_j^* \Omega L_z \psi_j + |\psi_j|^2 \sum_{l=1}^2 \beta_{jl} |\psi_l|^2 \right) - \lambda \psi_j \psi_{k_j}^* + \lambda \psi_j^* \psi_{k_j} \right] d\mathbf{x} \\ &= i\lambda \int_{\mathbb{R}^d} \left( \psi_j^* \psi_{k_j} - \psi_j \psi_{k_j}^* \right) d\mathbf{x} = 2\lambda \text{Re} \left[ \int_{\mathbb{R}^d} i \psi_j^* \psi_{k_j} d\mathbf{x} \right], \quad t \geq 0. \end{aligned} \quad (4.4)$$

Similarly, differentiating (4.4) with respect to  $t$ , noting (2.9) and integrating by parts, we get

$$\begin{aligned} N_j''(t) &= 2\lambda \frac{d}{dt} \text{Re} \left[ \int_{\mathbb{R}^d} i \psi_j^* \psi_{k_j} d\mathbf{x} \right] = 2\lambda \text{Re} \left[ \int_{\mathbb{R}^d} \left( i \psi_{k_j} \partial_t \psi_j^* + i \psi_j^* \partial_t \psi_{k_j} \right) d\mathbf{x} \right] \\ &= 2\lambda \text{Re} \left[ \int_{\mathbb{R}^d} \left[ \psi_{k_j} \left( \frac{1}{2} \nabla^2 \psi_j^* - V_j(\mathbf{x}) \psi_j^* + \Omega L_z^* \psi_j^* + \lambda \psi_{k_j}^* - \psi_j^* \sum_{l=1}^2 \beta_{jl} |\psi_l|^2 \right) \right. \right. \\ &\quad \left. \left. + \psi_j^* \left( -\frac{1}{2} \nabla^2 \psi_{k_j} + V_{k_j}(\mathbf{x}) \psi_{k_j} - \Omega L_z \psi_{k_j} - \lambda \psi_j + \psi_{k_j} \sum_{l=1}^2 \beta_{k_j l} |\psi_l|^2 \right) \right] d\mathbf{x} \right] \\ &= \lambda \int_{\mathbb{R}^d} \left[ \left( \psi_j^* \psi_{k_j} + \psi_j \psi_{k_j}^* \right) \left( V_{k_j}(\mathbf{x}) - V_j(\mathbf{x}) - (\beta_{jj} - \beta_{k_j k_j}) |\psi_j|^2 \right. \right. \\ &\quad \left. \left. + (\beta_{k_j k_j} - \beta_{j k_j}) |\psi_{k_j}|^2 \right) - 2\lambda \left( |\psi_j|^2 - |\psi_{k_j}|^2 \right) \right] d\mathbf{x}, \quad t \geq 0. \end{aligned} \quad (4.5)$$

Thus the Eq. (4.1) is a combination of (4.5) and (2.12). In addition, the initial conditions (4.2) and (4.3) can be obtained from (2.13) and (4.4) by setting  $t = 0$ , respectively.  $\square$

**Lemma 4.2.** (i) If the external trapping potentials are the same and the inter/intra-component  $s$ -wave scattering lengths in (2.9) are the same, i.e.

$$V_1(\mathbf{x}) = V_2(\mathbf{x}) \quad \mathbf{x} \in \mathbb{R}^d, \quad \text{and} \quad \beta_{11} = \beta_{12} = \beta_{22} \quad (\text{i.e. } a_{11} = a_{12} = a_{22}), \quad (4.6)$$

for any initial data  $(\psi_1^0(\mathbf{x}), \psi_2^0(\mathbf{x}))$ , we have, for  $t \geq 0$ ,

$$N_j(t) = \|\psi_j(\cdot, t)\|^2 = \left( N_j^{(0)} - \frac{1}{2} \right) \cos(2\lambda t) + \frac{N_j^{(1)}}{2\lambda} \sin(2\lambda t) + \frac{1}{2}, \quad j = 1, 2. \quad (4.7)$$

Thus in this case, the density of each component is a periodic function with period  $T = \pi/|\lambda|$  depending only on  $\lambda$ .

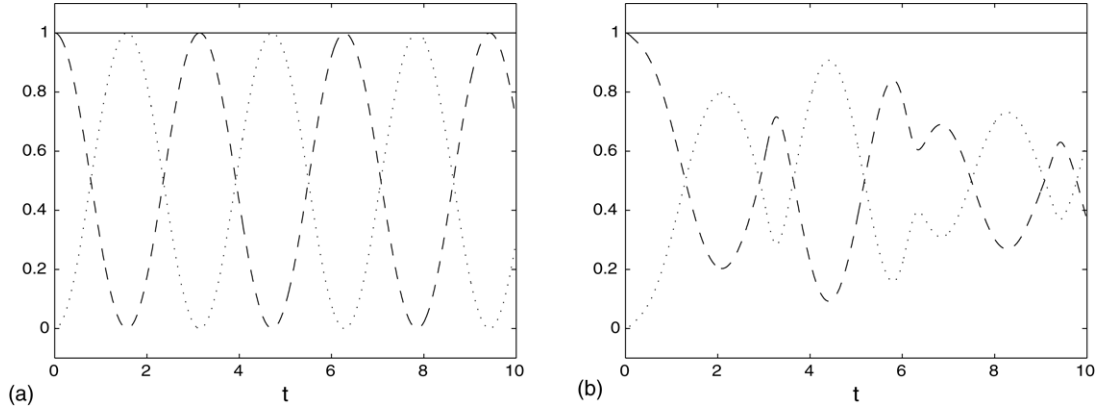


Fig. 3. Time evolution of the densities  $N_1(t) = \|\psi_1(\cdot, t)\|^2$  (dash line),  $N_2(t) = \|\psi_2(\cdot, t)\|^2$  (dot line) and  $N(t) = N_1(t) + N_2(t)$  (solid line) for two sets of interaction parameters: (a)  $\beta_{11} = \beta_{12} = \beta_{22}$ ; (b)  $\beta_{11} \neq \beta_{12} \neq \beta_{22}$ .

(ii) For all other cases, we have, for any  $t \geq 0$ ,

$$N_j(t) = \left( N_j^{(0)} - \frac{1}{2} \right) \cos(2\lambda t) + \frac{N_j^{(1)}}{2\lambda} \sin(2\lambda t) + \frac{1}{2} + f_j(t), \quad j = 1, 2, \tag{4.8}$$

where  $f_j(t)$  is the solution of the following second-order ODE:

$$f_j''(t) + 4\lambda^2 f_j(t) = F_j(t), \quad f_j(0) = f_j'(0) = 0. \tag{4.9}$$

**Proof.** (i) Under the assumptions in (i), the ODE (4.1) collapses to

$$N_j''(t) = -2\lambda^2 (2N_j(t) - 1), \quad t \geq 0, j = 1, 2. \tag{4.10}$$

Thus, (4.7) is the unique solution of the second-order ODE (4.10) with the initial data (4.2) and (4.3).

(ii) From the results in (i) and using the superposition principle, we get that (4.8) is the unique solution of the second-order ODE (4.1) with the initial data (4.2) and (4.3).  $\square$

To verify the dynamics of the densities  $N_j(t) = \|\psi_j(\cdot, t)\|^2$  ( $j = 1, 2$ ) in (4.7) and (4.8), we take  $\lambda = 1$ ,  $\Omega = 0.6$ ,  $\gamma_{x,j} = \gamma_{y,j} = 1$  ( $j = 1, 2$ ) in (2.9). The initial data in (2.10) is chosen as

$$\psi_1^0(\mathbf{x}) = \frac{x + iy}{\sqrt{\pi}} \exp\left(-\frac{x^2 + y^2}{2}\right), \quad \psi_2^0(\mathbf{x}) \equiv 0, \quad \mathbf{x} \in \mathbb{R}^2. \tag{4.11}$$

Fig. 3 shows the time evolution of the densities for two sets of interaction parameters: (i)  $\beta_{11} = \beta_{12} = \beta_{22} = 500$  (i.e.  $a_{11}:a_{12}:a_{22} = 1:1:1$ ); (ii)  $\beta_{11} = 500$ ,  $\beta_{12} = 300$  and  $\beta_{22} = 400$  (i.e.  $a_{11}:a_{12}:a_{22} = 1:0.6:0.8$ ).

From Fig. 3, we can see that (i) the total density  $N(t)$  is conserved in the discrete level for both cases; (ii) the densities of both components, i.e.  $N_1(t)$  and  $N_2(t)$ , are periodic functions of period  $T = \pi/\lambda = \pi$  when  $\beta_{11} = \beta_{12} = \beta_{22}$  (cf. Fig. 3(a)); otherwise when  $\beta_{11} \neq \beta_{12} \neq \beta_{22}$  they are periodic functions of period  $T = \pi$  with a perturbation (cf. Fig. 3(b)), which confirms the analytical results in (4.7) and (4.8).

#### 4.2. Conservation of angular momentum expectation

As a measure of vortex flux, we define the total angular momentum expectation:

$$\langle L_z \rangle(t) = \langle L_z \rangle_1(t) + \langle L_z \rangle_2(t), \quad t \geq 0, \tag{4.12}$$

where for  $j = 1, 2$

$$\langle L_z \rangle_j(t) = \int_{\mathbb{R}^d} \psi_j^*(\mathbf{x}, t) L_z \psi_j(\mathbf{x}, t) d\mathbf{x} = i \int_{\mathbb{R}^d} \psi_j^*(\mathbf{x}, t) (y \partial_x - x \partial_y) \psi_j(\mathbf{x}, t) d\mathbf{x}. \tag{4.13}$$

In fact,  $\langle \tilde{L}_z \rangle_j(t) := \frac{\langle L_z \rangle_j(t)}{N_j(t)}$  is the angular momentum expectation of the  $j$ th ( $j = 1, 2$ ) component. Typically when  $\lambda = 0$ , as the density of each component is conserved, then  $\langle \tilde{L}_z \rangle_j(t) = \frac{\langle L_z \rangle_j(t)}{N_j(0)}$ . For the dynamics of the angular momentum expectations in rotating two-component BEC, we have the following lemmas.

**Lemma 4.3.** Suppose  $(\psi_1(\mathbf{x}, t), \psi_2(\mathbf{x}, t))$  is the solution of the CGPEs (2.9)–(2.10); then we have,

$$\begin{aligned} \frac{d\langle L_z \rangle_j(t)}{dt} &= (\gamma_{x,j}^2 - \gamma_{y,j}^2) \int_{\mathbb{R}^d} xy |\psi_j|^2 d\mathbf{x} - \beta_{jk_j} \int_{\mathbb{R}^d} |\psi_j|^2 (x \partial_y - y \partial_x) |\psi_{k_j}|^2 d\mathbf{x} \\ &\quad - 2\lambda \operatorname{Re} \left[ \int_{\mathbb{R}^d} \psi_{k_j}^* (x \partial_y - y \partial_x) \psi_j d\mathbf{x} \right], \quad t \geq 0, j = 1, 2. \end{aligned} \quad (4.14)$$

**Proof.** Differentiating (4.13) with respect to  $t$ , noting (2.7) and (2.9), and integrating by parts, we obtain for  $j = 1, 2$

$$\begin{aligned} \frac{d\langle L_z \rangle_j(t)}{dt} &= \int_{\mathbb{R}^d} \left[ \partial_t \psi_j^* L_z \psi_j + \psi_j^* L_z \partial_t \psi_j \right] d\mathbf{x} = \int_{\mathbb{R}^d} \left[ -i \partial_t \psi_j^* \widehat{L}_z \psi_j + i \partial_t \psi_j \widehat{L}_z \psi_j^* \right] d\mathbf{x} \\ &= \int_{\mathbb{R}^d} \left[ \widehat{L}_z \psi_j \left( -\frac{1}{2} \nabla^2 \psi_j^* + V_j(\mathbf{x}) \psi_j^* - \Omega L_z^* \psi_j^* + \psi_j^* \sum_{l=1}^2 \beta_{jl} |\psi_l|^2 - \lambda \psi_{k_j}^* \right) \right. \\ &\quad \left. + \widehat{L}_z \psi_j^* \left( -\frac{1}{2} \nabla^2 \psi_j + V_j(\mathbf{x}) \psi_j - \Omega L_z \psi_j + \psi_j \sum_{l=1}^2 \beta_{jl} |\psi_l|^2 - \lambda \psi_{k_j} \right) \right] d\mathbf{x} \\ &= \int_{\mathbb{R}^d} \left[ -\frac{1}{2} \left( \widehat{L}_z \psi_j \nabla^2 \psi_j^* + \widehat{L}_z \psi_j^* \nabla^2 \psi_j \right) + V_j(\mathbf{x}) \left( \psi_j^* \widehat{L}_z \psi_j + \psi_j \widehat{L}_z \psi_j^* \right) \right. \\ &\quad \left. + \left( \psi_j^* \widehat{L}_z \psi_j + \psi_j \widehat{L}_z \psi_j^* \right) \left( \beta_{jj} |\psi_j|^2 + \beta_{jk_j} |\psi_{k_j}|^2 \right) - \lambda \left( \psi_{k_j}^* \widehat{L}_z \psi_j + \psi_{k_j} \widehat{L}_z \psi_j^* \right) \right] d\mathbf{x} \\ &= \int_{\mathbb{R}^d} \left[ (\gamma_{x,j}^2 - \gamma_{y,j}^2) xy |\psi_j|^2 - \beta_{jk_j} |\psi_j|^2 \widehat{L}_z |\psi_{k_j}|^2 - 2\lambda \operatorname{Re} \left( \psi_{k_j}^* \widehat{L}_z \psi_j \right) \right] d\mathbf{x}. \end{aligned} \quad (4.15)$$

Then the equality (4.14) is a combination of (2.7) and (4.15).  $\square$

**Lemma 4.4.** Suppose the traps in (2.11) are radially symmetric in 2D, and resp. cylindrically symmetric in 3D, i.e.  $\gamma_{x,1} = \gamma_{y,1}$  and  $\gamma_{x,2} = \gamma_{y,2}$ .

(i) For any given initial data  $(\psi_1^0(\mathbf{x}), \psi_2^0(\mathbf{x}))$  in (2.10), the total angular momentum expectation is conserved, i.e.

$$\langle L_z \rangle(t) \equiv \langle L_z \rangle(0) = \sum_{j=1}^2 \int_{\mathbb{R}^d} \left( \psi_j^0(\mathbf{x}) \right)^* L_z \psi_j^0(\mathbf{x}) d\mathbf{x}, \quad t \geq 0. \quad (4.16)$$

In addition, the energy for non-rotating part is also conserved, i.e.

$$\begin{aligned} E_n(\psi_1, \psi_2) &:= \int_{\mathbb{R}^d} \left[ \sum_{j=1}^2 \left( \frac{1}{2} |\nabla \psi_j|^2 + V_j(\mathbf{x}) |\psi_j|^2 + \sum_{l=1}^2 \frac{\beta_{jl}}{2} |\psi_j|^2 |\psi_l|^2 \right) - 2\lambda \operatorname{Re}(\psi_1^* \psi_2) \right] d\mathbf{x} \equiv E_n(\psi_1^0, \psi_2^0), \\ &t \geq 0. \end{aligned} \quad (4.17)$$

(ii) Suppose the initial data  $(\psi_1^0(\mathbf{x}), \psi_2^0(\mathbf{x}))$  in (2.10) is chosen as

$$\psi_j^0(\mathbf{x}) = f_j(r) e^{im_j \theta} \quad \text{with } m_j \in \mathbb{Z} \quad \text{and} \quad f_j(0) = 0 \quad \text{when } m_j \neq 0, \quad (4.18)$$

in 2D, and resp. in 3D,

$$\psi_j^0(\mathbf{x}) = f_j(r, z) e^{im_j \theta} \quad \text{with } m_j \in \mathbb{Z} \quad \text{and} \quad f_j(0, z) = 0 \quad \text{when } m_j \neq 0. \quad (4.19)$$

If  $\lambda = 0$ , then  $\langle \widetilde{L}_z \rangle_1(t)$  and  $\langle \widetilde{L}_z \rangle_2(t)$  are conserved, i.e.

$$\langle \widetilde{L}_z \rangle_j(t) \equiv \langle \widetilde{L}_z \rangle_j(0) = \frac{1}{N_j(0)} \int_{\mathbb{R}^d} \left( \psi_j^0(\mathbf{x}) \right)^* L_z \psi_j^0(\mathbf{x}) d\mathbf{x}, \quad t \geq 0, j = 1, 2. \quad (4.20)$$

On the other hand, if  $m_1 = m_2 := m$  in (4.18) for 2D, and resp. in (4.19) for 3D, then for any given  $\lambda$ ,  $\langle \widetilde{L}_z \rangle_1(t)$  and  $\langle \widetilde{L}_z \rangle_2(t)$  are conserved, i.e.

$$\langle \widetilde{L}_z \rangle_j(t) \equiv \langle \widetilde{L}_z \rangle_j(0) = m, \quad t \geq 0, j = 1, 2. \quad (4.21)$$

**Proof.** (i) Summing (4.14) for  $j = 1, 2$ , noting (4.12) and (2.3), and integrating by parts, we have

$$\begin{aligned} \frac{d\langle L_z \rangle(t)}{dt} &= \sum_{j=1}^2 (\gamma_{x,j}^2 - \gamma_{y,j}^2) \int_{\mathbb{R}^d} xy |\psi_j|^2 d\mathbf{x} - 2\lambda \operatorname{Re} \left[ \int_{\mathbb{R}^d} (\psi_2^* \widehat{L}_z \psi_1 + \psi_1^* \widehat{L}_z \psi_2) d\mathbf{x} \right] \\ &\quad - \beta_{12} \int_{\mathbb{R}^d} (|\psi_1|^2 \widehat{L}_z |\psi_2|^2 + |\psi_2|^2 \widehat{L}_z |\psi_1|^2) d\mathbf{x} \\ &= \sum_{j=1}^2 (\gamma_{x,j}^2 - \gamma_{y,j}^2) \int_{\mathbb{R}^d} xy |\psi_j|^2 d\mathbf{x}, \quad t \geq 0. \end{aligned} \quad (4.22)$$

Consequently, if  $\gamma_{x,1} = \gamma_{y,1}$  and  $\gamma_{x,2} = \gamma_{y,2}$ , (4.22) reduces to the first-order ODE:

$$\frac{d\langle L_z \rangle(t)}{dt} = 0, \quad t \geq 0. \quad (4.23)$$

We thus get the conservation of the total angular momentum expectation  $\langle L_z \rangle$  immediately.

Noting  $E(\psi_1, \psi_2) = E_n(\psi_1, \psi_2) - \Omega \operatorname{Re}(\langle L_z \rangle)$  and  $\operatorname{Re}(\langle L_z \rangle) = \langle L_z \rangle$ , we get (4.17) from (2.14) and (4.16).

(ii) When the initial data  $(\psi_1^0(\mathbf{x}), \psi_2^0(\mathbf{x}))$  in (2.10) satisfies (4.18) for 2D, and resp. (4.19) for 3D, due to symmetry, when  $\lambda = 0$  or  $m_1 = m_2$ , the solution  $(\psi_1(\mathbf{x}, t), \psi_2(\mathbf{x}, t))$  of (2.9)–(2.10) satisfies

$$\psi_j(\mathbf{x}, t) = g_j(r, t) e^{im_j \theta} \quad \text{with } g_j(r, 0) = f_j(r), \quad (4.24)$$

in 2D, and resp. in 3D,

$$\psi_j(\mathbf{x}, t) = g_j(r, z, t) e^{im_j \theta} \quad \text{with } g_j(r, z, 0) = f_j(r, z). \quad (4.25)$$

Plugging (4.24) or (4.25) into (4.14) and noting  $\lambda = 0$ , we obtain for  $j = 1, 2$

$$\begin{aligned} \frac{d\langle L_z \rangle_j(t)}{dt} &= -\beta_{jkj} \int_{\mathbb{R}^d} |\psi_j|^2 \partial_\theta |\psi_{k_j}|^2 d\mathbf{x} = -\beta_{jkj} \int_{\mathbb{R}^d} |g_j|^2 \partial_\theta |g_{k_j}|^2 d\mathbf{x} \\ &= 0, \quad t \geq 0. \end{aligned} \quad (4.26)$$

We thus get the conservation of  $(\widetilde{L}_z)_j(t)$  ( $j = 1, 2$ ) from (4.26) and (2.15) immediately. On the other hand, when  $m_1 = m_2 := m$  in (4.24) for 2D, and resp. (4.25) for 3D, noting (2.7), we have, for  $j = 1, 2$

$$\begin{aligned} \langle \widetilde{L}_z \rangle_j(t) &= \frac{\langle L_z \rangle_j(t)}{N_j(t)} = \frac{\int_{\mathbb{R}^d} \psi_j^* L_z \psi_j d\mathbf{x}}{\int_{\mathbb{R}^d} |\psi_j|^2 d\mathbf{x}} = \frac{-i \int_{\mathbb{R}^d} \psi_j^* \partial_\theta \psi_j d\mathbf{x}}{\int_{\mathbb{R}^d} |\psi_j|^2 d\mathbf{x}} \\ &= \frac{-i \int_{\mathbb{R}^d} g_j^* e^{-im\theta} (im) g_j e^{im\theta} d\mathbf{x}}{\int_{\mathbb{R}^d} |g_j|^2 d\mathbf{x}} = m \frac{\int_{\mathbb{R}^d} |g_j|^2 d\mathbf{x}}{\int_{\mathbb{R}^d} |g_j|^2 d\mathbf{x}} \equiv m, \quad t \geq 0. \end{aligned} \quad (4.27)$$

This immediately implies the conservation laws in (4.21).  $\square$

To verify the conservation of the angular momentum expectation, we take  $\Omega = 0.6$ ,  $\lambda = 1$ ,  $\beta_{11} = 400$ ,  $\beta_{12} = 388$  and  $\beta_{22} = 376$  in (2.9). The initial data in (2.10) is chosen as

$$\psi_j^0(\mathbf{x}) = \frac{x + iy}{\sqrt{2\pi}} \exp\left(-\frac{x^2 + y^2}{2}\right), \quad \mathbf{x} \in \mathbb{R}^2, j = 1, 2. \quad (4.28)$$

Fig. 4 shows time evolution of the angular momentum expectations for two sets of parameters: (i)  $\gamma_{x,1} = \gamma_{y,1} = \gamma_{x,2} = \gamma_{y,2} = 1$  which corresponds to a symmetric trap; (ii)  $\gamma_{x,1} = \gamma_{y,1} = 1$ ,  $\gamma_{x,2} = 1.05$ ,  $\gamma_{y,2} = 0.9$  which corresponds to an asymmetric trap.

From Fig. 4, we can see that (i) the total angular momentum expectation  $\langle L_z \rangle(t)$  is conserved when both of the two external trapping potentials are symmetric; furthermore, if the initial data satisfies (4.18), the quantities  $\langle \widetilde{L}_z \rangle_1(t)$  and  $\langle \widetilde{L}_z \rangle_2(t)$  are also conserved when  $m_1 = m_2$  (cf. Fig. 4(a)); (ii) if one or two of the external trapping potentials are asymmetric, the angular momentum expectations  $\langle L_z \rangle(t)$ ,  $\langle \widetilde{L}_z \rangle_1(t)$  and  $\langle \widetilde{L}_z \rangle_2(t)$  are not conserved (cf. Fig. 4(b)); (iii) all the above numerical results confirm the analytical result (4.16), (4.20) and (4.21).

### 4.3. Dynamics of condensate widths

Another important quantity characterizing the dynamics of a rotating two-component BEC is the condensate width defined as

$$\sigma_\alpha(t) = \sqrt{\delta_\alpha(t)} = \sqrt{\delta_{\alpha,1}(t) + \delta_{\alpha,2}(t)}, \quad \alpha = x, y \text{ or } z, \quad (4.29)$$

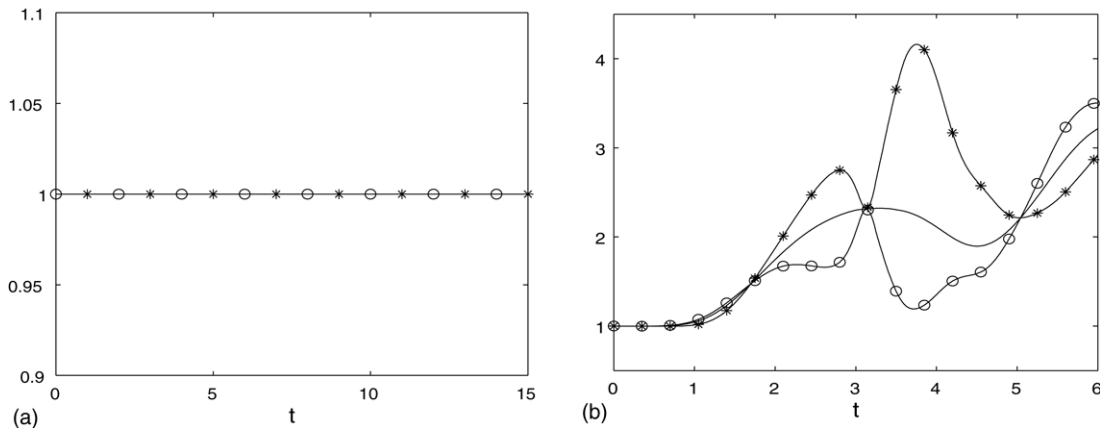


Fig. 4. Time evolution of the angular momentum expectations  $\langle L_z \rangle(t)$  (solid line),  $\langle \tilde{L}_z \rangle_1(t)$  ('-\*') and  $\langle \tilde{L}_z \rangle_2(t)$  ('-o'): (a) for case (i); (b) for case (ii).

where

$$\delta_{\alpha,j}(t) = \langle \alpha^2 \rangle_j(t) = \int_{\mathbb{R}^d} \alpha^2 |\psi_j(\mathbf{x}, t)|^2 d\mathbf{x}, \quad t \geq 0, j = 1, 2. \quad (4.30)$$

For the dynamics of condensate widths, we have the following lemmas.

**Lemma 4.5.** Suppose  $(\psi_1(\mathbf{x}, t), \psi_2(\mathbf{x}, t))$  is the solution of problem (2.9)–(2.10); then we have

$$\begin{aligned} \frac{d^2 \delta_\alpha(t)}{dt^2} &= \int_{\mathbb{R}^d} \sum_{j=1}^2 \left[ (\partial_y \alpha - \partial_x \alpha) \left( 4i\Omega \psi_j^* (x\partial_y + y\partial_x) \psi_j + 2\Omega^2 (x^2 - y^2) |\psi_j|^2 \right) \right. \\ &\quad \left. + 2|\partial_\alpha \psi_j|^2 - 2\alpha |\psi_j|^2 \partial_\alpha (V_j(\mathbf{x})) + |\psi_j|^2 \sum_{l=1}^2 \beta_{jl} |\psi_l|^2 \right] d\mathbf{x}, \quad t \geq 0, \end{aligned} \quad (4.31)$$

$$\delta_\alpha(0) = \delta_\alpha^{(0)} = \int_{\mathbb{R}^d} \alpha^2 (|\psi_1^0(\mathbf{x})|^2 + |\psi_2^0(\mathbf{x})|^2) d\mathbf{x}, \quad \alpha = x, y, z, \quad (4.32)$$

$$\delta'_\alpha(0) = \delta_\alpha^{(1)} = 2 \sum_{j=1}^2 \int_{\mathbb{R}^d} \alpha \left[ -\Omega |\psi_j^0|^2 (x\partial_y - y\partial_x) \alpha + \text{Im} \left( (\psi_j^0)^* \partial_\alpha \psi_j^0 \right) \right] d\mathbf{x}. \quad (4.33)$$

**Proof.** Differentiating (4.30) with respect to  $t$ , applying (2.9) and integration by parts, we obtain

$$\begin{aligned} \frac{d\delta_{\alpha,j}(t)}{dt} &= \frac{d}{dt} \int_{\mathbb{R}^d} \alpha^2 |\psi_j(\mathbf{x}, t)|^2 d\mathbf{x} = \int_{\mathbb{R}^d} \alpha^2 \left( \psi_j \partial_t \psi_j^* + \psi_j^* \partial_t \psi_j \right) d\mathbf{x} \\ &= \int_{\mathbb{R}^d} \left[ \frac{i}{2} \alpha^2 \left( \psi_j^* \nabla^2 \psi_j - \psi_j \nabla^2 \psi_j^* \right) + \Omega \alpha^2 (x\partial_y - y\partial_x) |\psi_j|^2 + i\lambda \alpha^2 \left( \psi_j^* \psi_{k_j} - \psi_j \psi_{k_j}^* \right) \right] d\mathbf{x} \\ &= \int_{\mathbb{R}^d} \left[ i\alpha \left( \psi_j \partial_\alpha \psi_j^* - \psi_j^* \partial_\alpha \psi_j \right) - 2\Omega \alpha |\psi_j|^2 (x\partial_y - y\partial_x) \alpha + i\lambda \alpha^2 \left( \psi_j^* \psi_{k_j} - \psi_j \psi_{k_j}^* \right) \right] d\mathbf{x}, \quad j = 1, 2. \end{aligned} \quad (4.34)$$

Differentiating the above equation again, applying (2.9) and integrating by parts, we get

$$\begin{aligned} \frac{d^2 \delta_{\alpha,j}(t)}{dt^2} &= \int_{\mathbb{R}^d} \left[ 2i\alpha \left( \partial_t \psi_j \partial_\alpha \psi_j^* - \partial_t \psi_j^* \partial_\alpha \psi_j \right) + i \left( \psi_j^* \partial_t \psi_j - \psi_j \partial_t \psi_j^* \right) \right. \\ &\quad \left. - 2\Omega \alpha \left( \psi_j \partial_t \psi_j^* + \psi_j^* \partial_t \psi_j \right) (x\partial_y - y\partial_x) \alpha + i\lambda \alpha^2 \left( \partial_t \psi_j^* \psi_{k_j} - \partial_t \psi_j \psi_{k_j}^* + \psi_j^* \partial_t \psi_{k_j} - \psi_j \partial_t \psi_{k_j}^* \right) \right] d\mathbf{x} \\ &:= I + II + III + IV, \quad j = 1, 2. \end{aligned} \quad (4.35)$$

Plugging (2.9) into (4.35), noting (2.3) and integrating by parts, we obtain

$$\begin{aligned}
 I &:= \int_{\mathbb{R}^d} 2\alpha \left[ (i\partial_t \psi_j) \partial_\alpha \psi_j^* + (-i\partial_t \psi_j^*) \partial_\alpha \psi_j \right] \mathbf{d}\mathbf{x} \\
 &= \int_{\mathbb{R}^d} \left[ -\alpha \left( \partial_\alpha \psi_j^* \nabla^2 \psi_j + \partial_\alpha \psi_j \nabla^2 \psi_j^* \right) - 2\Omega\alpha \left( \partial_\alpha \psi_j^* L_z \psi_j + \partial_\alpha \psi_j L_z^* \psi_j^* \right) \right. \\
 &\quad \left. + 2\alpha \left( V_j(\mathbf{x}) + \sum_{l=1}^2 \beta_{jl} |\psi_l|^2 \right) \left( \psi_j \partial_\alpha \psi_j^* + \psi_j^* \partial_\alpha \psi_j \right) - 4\lambda\alpha \operatorname{Re} \left( \psi_{k_j} \partial_\alpha \psi_j^* \right) \right] \mathbf{d}\mathbf{x} \\
 &= \int_{\mathbb{R}^d} \left[ -|\nabla \psi_j|^2 + 2|\partial_\alpha \psi_j|^2 - 2V_j(\mathbf{x})|\psi_j|^2 - 2\alpha|\psi_j|^2 \partial_\alpha (V_j(\mathbf{x})) - \beta_{jj} |\psi_j|^4 \right. \\
 &\quad \left. + 2\beta_{jk_j} \alpha |\psi_{k_j}|^2 \partial_\alpha |\psi_j|^2 - 2\lambda\alpha \left( \psi_{k_j} \partial_\alpha \psi_j^* + \psi_{k_j}^* \partial_\alpha \psi_j \right) + 2\Omega\psi_j^* L_z \psi_j \right. \\
 &\quad \left. + 2i\Omega (\partial_y \alpha - \partial_x \alpha) \psi_j^* (x\partial_y + y\partial_x) \psi_j \right] \mathbf{d}\mathbf{x}. \\
 II &:= \int_{\mathbb{R}^d} \left[ \psi_j^* (i\partial_t \psi_j) + (-i\partial_t \psi_j^*) \psi_j \right] \mathbf{d}\mathbf{x} \\
 &= \int_{\mathbb{R}^d} \left[ -\frac{1}{2} \left( \psi_j^* \nabla^2 \psi_j + \psi_j \nabla^2 \psi_j^* \right) + 2V_j(\mathbf{x})|\psi_j|^2 - \Omega \left( \psi_j^* L_z \psi_j + \psi_j L_z^* \psi_j^* \right) \right. \\
 &\quad \left. - \lambda \left( \psi_j^* \psi_{k_j} + \psi_j \psi_{k_j}^* \right) + 2|\psi_j|^2 \sum_{l=1}^2 \beta_{jl} |\psi_l|^2 \right] \mathbf{d}\mathbf{x} \\
 &= 2 \int_{\mathbb{R}^d} \left[ \frac{1}{2} |\nabla \psi_j|^2 + V_j(\mathbf{x})|\psi_j|^2 - \Omega\psi_j^* L_z \psi_j + \sum_{l=1}^2 \beta_{jl} |\psi_j|^2 |\psi_l|^2 - \lambda \operatorname{Re} \left( \psi_j^* \psi_{k_j} \right) \right] \mathbf{d}\mathbf{x}. \\
 III &:= -2\Omega \int_{\mathbb{R}^d} \alpha L_z \alpha \left[ \psi_j^* (i\partial_t \psi_j) - (-i\partial_t \psi_j^*) \psi_j \right] \mathbf{d}\mathbf{x} \\
 &= 2\Omega \int_{\mathbb{R}^d} \alpha L_z \alpha \left[ -\frac{1}{2} \left( \psi_j \nabla^2 \psi_j^* - \psi_j^* \nabla^2 \psi_j \right) + \Omega \left( \psi_j L_z \psi_j^* - \psi_j^* L_z^* \psi_j \right) + \lambda \left( \psi_j \psi_{k_j}^* - \psi_j^* \psi_{k_j} \right) \right] \mathbf{d}\mathbf{x} \\
 &= 2\Omega \int_{\mathbb{R}^d} (\partial_y \alpha - \partial_x \alpha) \left[ i\psi_j^* (x\partial_y + y\partial_x) \psi_j + \Omega |\psi_j|^2 (x^2 - y^2) - i\lambda xy \left( \psi_j^* \psi_{k_j} - \psi_j \psi_{k_j}^* \right) \right] \mathbf{d}\mathbf{x}. \\
 IV &:= i\lambda \int_{\mathbb{R}^d} \alpha^2 \left( \partial_t \psi_j^* \psi_{k_j} - \partial_t \psi_j \psi_{k_j}^* + \psi_j^* \partial_t \psi_{k_j} - \psi_j \partial_t \psi_{k_j}^* \right) \mathbf{d}\mathbf{x}.
 \end{aligned}$$

Plugging I–IV into (4.35), we have, for  $j = 1, 2$

$$\begin{aligned}
 \frac{d^2 \delta_{\alpha,j}(t)}{dt^2} &= \int_{\mathbb{R}^d} \left[ (\partial_y \alpha - \partial_x \alpha) \left( 2\Omega^2 (x^2 - y^2) |\psi_j|^2 + 4i\Omega \psi_j^* (x\partial_y + y\partial_x) \psi_j \right) \right. \\
 &\quad \left. + 2|\partial_\alpha \psi_j|^2 - 2\alpha |\psi_j|^2 \partial_\alpha (V_j(\mathbf{x})) + \beta_{jj} |\psi_j|^4 - 2\beta_{jk_j} \alpha |\psi_j|^2 \partial_\alpha |\psi_{k_j}|^2 \right] \mathbf{d}\mathbf{x} \\
 &\quad - 2\lambda \int_{\mathbb{R}^d} \left[ \operatorname{Re} \left( \psi_j^* \psi_{k_j} \right) + 2\alpha \operatorname{Re} \left( \psi_{k_j} \partial_\alpha \psi_j^* \right) - \Omega xy (\partial_y \alpha - \partial_x \alpha) \operatorname{Re} \left( \psi_j^* \psi_{k_j} \right) \right] \mathbf{d}\mathbf{x} \\
 &\quad + i\lambda \int_{\mathbb{R}^d} \alpha^2 \left( \partial_t \psi_j^* \psi_{k_j} - \partial_t \psi_j \psi_{k_j}^* + \psi_j^* \partial_t \psi_{k_j} - \psi_j \partial_t \psi_{k_j}^* \right) \mathbf{d}\mathbf{x}. \tag{4.36}
 \end{aligned}$$

Thus the equality (4.31) can be obtained by summing (4.36) for  $j = 1, 2$  and noting (2.3). In addition, (4.32) and (4.33) can be obtained by summing (4.30) and (4.34) with  $t = 0$  for  $j = 1, 2$ , respectively.  $\square$

**Lemma 4.6.** *In 2D with radially symmetric traps, i.e.,  $d = 2$  and  $\gamma_{x,1} = \gamma_{y,1} = \gamma_{x,2} = \gamma_{y,2} := \gamma_r$  in (2.9), we have*

(i) *If there is no external driving field, i.e.  $\lambda = 0$  in (2.9), for any given initial data  $(\psi_1^0(\mathbf{x}), \psi_2^0(\mathbf{x}))$  in (2.10), we have, for  $t \geq 0$ ,*

$$\delta_r(t) = \frac{E(\psi_1^0, \psi_2^0) + \Omega \langle L_z \rangle(0)}{\gamma_r^2} [1 - \cos(2\gamma_r t)] + \delta_r^{(0)} \cos(2\gamma_r t) + \frac{\delta_r^{(1)}}{2\gamma_r} \sin(2\gamma_r t), \tag{4.37}$$

where  $\delta_r(t) = \delta_x(t) + \delta_y(t)$ ,  $\delta_r^{(0)} := \delta_x(0) + \delta_y(0)$  and  $\delta_r^{(1)} := \delta'_x(0) + \delta'_y(0)$ . Furthermore, when the initial data  $(\psi_1^0(\mathbf{x}), \psi_2^0(\mathbf{x}))$  in (2.10) satisfies (4.18), we have, for  $t \geq 0$ ,

$$\begin{aligned}
 \delta_x(t) = \delta_y(t) &= \frac{1}{2} \delta_r(t) \\
 &= \frac{E(\psi_1^0, \psi_2^0) + \Omega \langle L_z \rangle(0)}{2\gamma_r^2} [1 - \cos(2\gamma_r t)] + \delta_x^{(0)} \cos(2\gamma_r t) + \frac{\delta_x^{(1)}}{2\gamma_r} \sin(2\gamma_r t). \tag{4.38}
 \end{aligned}$$

Thus in this case, the condensate widths  $\sigma_r(t)$ ,  $\sigma_x(t)$  and  $\sigma_y(t)$  are periodic functions with frequency doubling the trapping frequency.

(ii) If there is an external driving field, i.e.  $\lambda \neq 0$  in (2.9), we have

$$\delta_r(t) = \frac{E(\psi_1^0, \psi_2^0) + \Omega \langle L_z \rangle(0)}{\gamma_r^2} + \left( \delta_r^{(0)} - \frac{E(\psi_1^0, \psi_2^0) + \Omega \langle L_z \rangle(0)}{\gamma_r^2} \right) \cos(2\gamma_r t) + \frac{\delta_r^{(1)}}{2\gamma_r} \sin(2\gamma_r t) + g_r(t), \quad t \geq 0, \quad (4.39)$$

where  $g_r(t)$  is the solution of the following second-order ODE:

$$\frac{d^2 g_r(t)}{dt^2} + 4\gamma_r^2 g_r(t) = G_r(t), \quad g_r(0) = g_r'(0) = 0, \quad (4.40)$$

with

$$G_r(t) = 8\lambda \int_{\mathbb{R}^d} \operatorname{Re}(\psi_1^* \psi_2) \, d\mathbf{x}.$$

**Proof.** Summing (4.31) with  $d = 2$  and  $\gamma_{x,1} = \gamma_{y,1} = \gamma_{x,2} = \gamma_{y,2} := \gamma_r$  for  $\alpha = x$  and  $y$ , noting (2.14) and (4.16), we have the following ODE for  $\delta_r(t)$ :

$$\begin{aligned} \frac{d^2 \delta_r(t)}{dt^2} &= \int_{\mathbb{R}^d} \sum_{j=1}^2 \left[ 2|\nabla \psi_j|^2 - 2|\psi_j|^2 (x\partial_x(V_j(\mathbf{x})) + y\partial_y(V_j(\mathbf{x}))) + 2|\psi_j|^2 \sum_{l=1}^2 \beta_{jl} |\psi_l|^2 \right] d\mathbf{x} \\ &= - \int_{\mathbb{R}^d} \left[ \sum_{j=1}^2 (8V_j(\mathbf{x})|\psi_j|^2 - 4\Omega \psi_j^* L_z \psi_j) - 4\lambda(\psi_1^* \psi_2 + \psi_1 \psi_2^*) \right] d\mathbf{x} + 4E(\psi_1(\cdot, t), \psi_2(\cdot, t)) \\ &= -4\gamma_r^2 \delta_r(t) + 4\Omega \langle L_z \rangle(t) + 4E(\psi_1(\cdot, t), \psi_2(\cdot, t)) + 8\lambda \int_{\mathbb{R}^d} \operatorname{Re}(\psi_1^* \psi_2) \, d\mathbf{x} \\ &= -4\gamma_r^2 \delta_r(t) + 4\Omega \langle L_z \rangle(0) + 4E(\psi_1^0, \psi_2^0) + 8\lambda \int_{\mathbb{R}^d} \operatorname{Re}(\psi_1^* \psi_2) \, d\mathbf{x}. \end{aligned} \quad (4.41)$$

(i) When  $\lambda = 0$ , the above ODE collapses to

$$\frac{d^2 \delta_r(t)}{dt^2} = -4\gamma_r^2 \delta_r(t) + 4\Omega \langle L_z \rangle(0) + 4E(\psi_1^0, \psi_2^0), \quad t \geq 0. \quad (4.42)$$

$$\delta_r(0) = \delta_r^{(0)}, \quad \delta_r'(0) = \delta_r^{(1)}. \quad (4.43)$$

Thus, (4.37) is the unique solution of the second-order ODE (4.42) with the initial data (4.43). Furthermore, when the initial data  $(\psi_1^0(\mathbf{x}), \psi_2^0(\mathbf{x}))$  in (2.10) satisfies (4.18), the solution  $(\psi_1(\mathbf{x}, t), \psi_2(\mathbf{x}, t))$  of (2.9)–(2.10) satisfies (4.24). This implies

$$\begin{aligned} \delta_x(t) &= \delta_{x,1}(t) + \delta_{x,2}(t) = \int_{\mathbb{R}^2} x^2 (|\psi_1(x, y, t)|^2 + |\psi_2(x, y, t)|^2) \, d\mathbf{x} \\ &= \int_0^\infty \int_0^{2\pi} r^2 \cos^2 \theta (|g_1(r, t)|^2 + |g_2(r, t)|^2) \, r \, d\theta \, dr \\ &= \pi \int_0^\infty r^2 (|g_1(r, t)|^2 + |g_2(r, t)|^2) \, r \, dr \\ &= \int_0^\infty \int_0^{2\pi} r^2 \sin^2 \theta (|g_1(r, t)|^2 + |g_2(r, t)|^2) \, r \, d\theta \, dr \\ &= \int_{\mathbb{R}^2} y^2 (|\psi_1(x, y, t)|^2 + |\psi_2(x, y, t)|^2) \, d\mathbf{x} = \delta_y(t), \quad t \geq 0. \end{aligned} \quad (4.44)$$

Therefore, (4.38) is a combination of (4.44) and (4.37).

(ii) When  $\lambda \neq 0$ , the ODE (4.41) collapses to

$$\frac{d^2 \delta_r(t)}{dt^2} = -4\gamma_r^2 \delta_r(t) + 4\Omega \langle L_z \rangle(0) + 4E(\psi_1^0, \psi_2^0) + G_r(t), \quad t \geq 0, \quad (4.45)$$

and (4.39) is the unique solution of the second-order ODE (4.45) with the initial data (4.43).  $\square$

To verify the dynamics of the condensate widths, we take  $\Omega = 0.6$ ,  $\lambda = 0$ ,  $\beta_{11} = 400$ ,  $\beta_{12} = 388$  and  $\beta_{22} = 376$  in (2.9). The initial data in (2.10) is chosen as (4.28). Fig. 5 shows the time evolution of the condensate width for two sets of trapping frequencies:

(i)  $\gamma_{x,1} = \gamma_{y,1} = \gamma_{x,2} = \gamma_{y,2} = 1$ ; (ii)  $\gamma_{x,1} = \gamma_{y,2} = 1$  and  $\gamma_{x,2} = \gamma_{y,1} = 1.2$ .

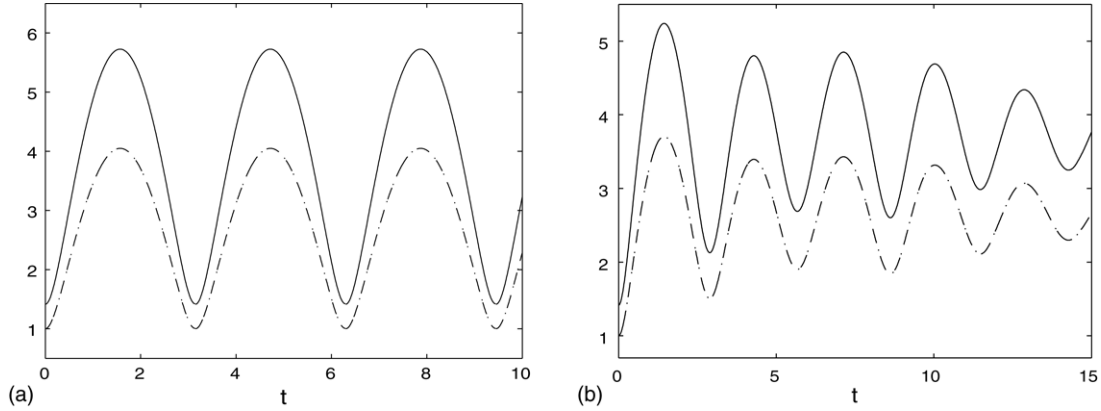


Fig. 5. Time evolution of the condensate widths  $\sigma_x(t)$  (dash line),  $\sigma_y(t)$  (dot line) and  $\sigma_r(t)$  (solid line) for two sets of trapping frequencies: (a) for case (i); (b) for case (ii).

From Fig. 5, we can see that the condensate widths  $\sigma_r(t)$ ,  $\sigma_x(t)$  and  $\sigma_y(t)$  are periodic functions of period  $T = \pi/\gamma_{x,1} = \pi$  when  $\gamma_{x,1} = \gamma_{y,1} = \gamma_{x,2} = \gamma_{y,2} = 1$  (cf. Fig. 5(a)) and periodic functions of period  $T = \pi$  with a perturbation when  $1 = \gamma_{x,1} = \gamma_{y,1} \neq \gamma_{x,2} = \gamma_{y,2} = 1.2$  (cf. Fig. 5(b)), again confirming the analytical results (4.38) and (4.39), respectively.

4.4. Dynamics of a stationary state with its centers shifted

When  $\lambda = 0$  in (2.9), let  $(\phi_1^e(\mathbf{x}), \phi_2^e(\mathbf{x}))$  be a stationary state of the CGPEs (2.9) with chemical potential  $(\mu_1^e, \mu_2^e)$ , i.e.,  $(\mu_1^e, \mu_2^e; \phi_1^e, \phi_2^e)$  satisfying

$$\mu_j^e \phi_j^e(\mathbf{x}) = -\frac{1}{2} \nabla^2 \phi_j^e + V_j(\mathbf{x}) \phi_j^e - \Omega L_z \phi_j^e + \sum_{l=1}^2 \beta_{jl} |\phi_l^e|^2 \phi_j^e, \quad \mathbf{x} \in \mathbb{R}^d, \tag{4.46}$$

$$\|\phi_j^e\|^2 := \int_{\mathbb{R}^d} |\phi_j^e(\mathbf{x})|^2 d\mathbf{x} = \frac{N_j^0}{N}, \quad j = 1, 2. \tag{4.47}$$

If the initial data  $(\psi_1^0(\mathbf{x}), \psi_2^0(\mathbf{x}))$  in (2.10) is chosen as a stationary state with a shift in its center, one can construct an exact solution of the CGPEs (2.9) with harmonic oscillator potentials (2.11). This kind of analytical construction can be used, in particular, in the benchmark and validation of numerical algorithms for the CGPEs (2.9). For single-component non-rotating and rotating BEC, this kind of analytical construction can be found in the literature [18,5]. For rotating two-component BEC, we have the following lemma.

**Lemma 4.7.** *If the initial data  $(\psi_1^0(\mathbf{x}), \psi_2^0(\mathbf{x}))$  in (2.10) is chosen as*

$$\psi_1^0(\mathbf{x}) = \phi_1^e(\mathbf{x} - \mathbf{x}_1^0), \quad \psi_2^0(\mathbf{x}) = \phi_2^e(\mathbf{x} - \mathbf{x}_2^0), \quad \mathbf{x} \in \mathbb{R}^d, \tag{4.48}$$

where  $\mathbf{x}_1^0$  and  $\mathbf{x}_2^0$  are two given points in  $\mathbb{R}^d$ , when  $\lambda = 0$ ,  $\mathbf{x}_1^0 = \mathbf{x}_2^0 := \mathbf{x}^0$  and  $V_1(\mathbf{x}) \equiv V_2(\mathbf{x})$ , then the exact solution of the CGPEs (2.9)–(2.10) satisfies

$$\psi_j(\mathbf{x}, t) = \phi_j^e(\mathbf{x} - \mathbf{x}(t)) e^{-i\mu_j^e t} e^{i w_j(\mathbf{x}, t)}, \quad \mathbf{x} \in \mathbb{R}^d, t \geq 0, j = 1, 2, \tag{4.49}$$

where for any  $t \geq 0$ ,  $w_j(\mathbf{x}, t)$  is a linear function for  $\mathbf{x}$ , i.e. for  $j = 1, 2$

$$w_j(\mathbf{x}, t) = \mathbf{c}_j(t) \cdot \mathbf{x} + g_j(t), \quad \mathbf{c}_j(t) = (c_{j,1}(t), \dots, c_{j,d}(t))^T, \quad \mathbf{x} \in \mathbb{R}^d, t \geq 0, \tag{4.50}$$

and  $\mathbf{x}(t)$  satisfies the following second-order ODE system

$$x''(t) - 2\Omega y'(t) + (\gamma_{x,1}^2 - \Omega^2) x(t) = 0, \tag{4.51}$$

$$y''(t) + 2\Omega x'(t) + (\gamma_{y,1}^2 - \Omega^2) y(t) = 0, \quad t \geq 0, \tag{4.52}$$

$$x(0) = x^0, \quad y(0) = y^0, \quad x'(0) = \Omega y^0, \quad y'(0) = -\Omega x^0. \tag{4.53}$$

Moreover, if in 3D, another ODE needs to be added:

$$z''(t) + \gamma_{z,1}^2 z(t) = 0, \quad z(0) = z^0, \quad z'(0) = 0. \tag{4.54}$$

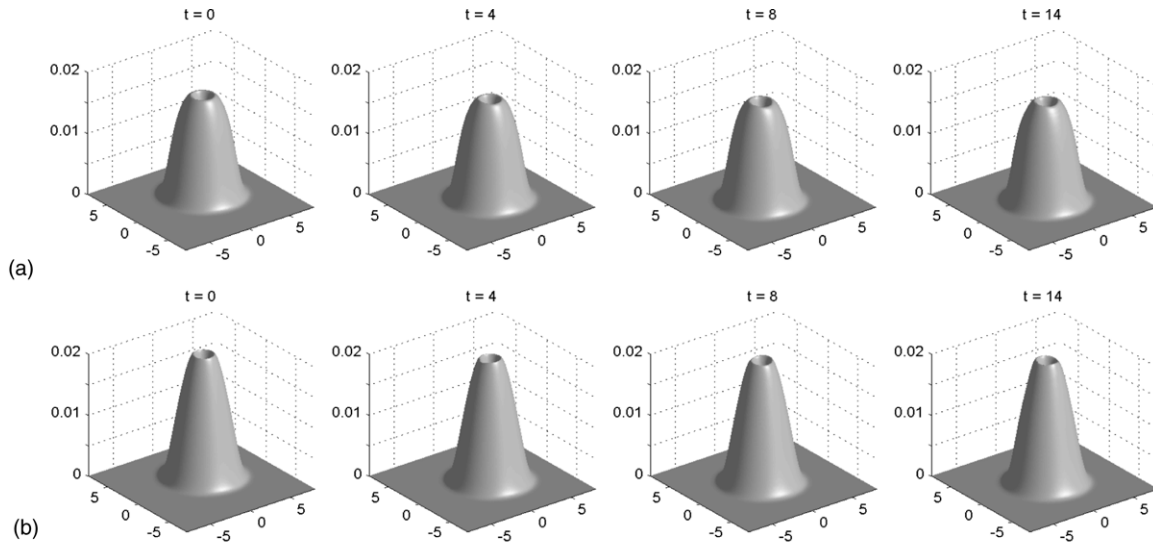


Fig. 6. Surface plots of the wave functions  $|\psi_1|^2$  (top row (a)) and  $|\psi_2|^2$  (bottom row (b)) at different times for case (i).

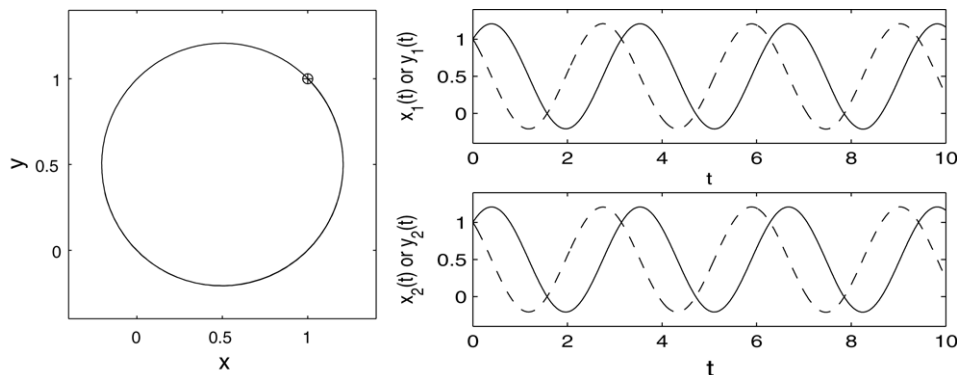


Fig. 7. Time evolution of the center of mass in (4.49), i.e.  $\mathbf{x}(t)$ , for case (i) ('+o': initial location of the two vortex centers  $\mathbf{x}_1^0/\mathbf{x}_2^0$  respectively).

**Proof.** The proof follows the line of the analogous result for rotating single-component BEC in [5].  $\square$

The ODE system (4.51)–(4.54) governing the motion of the center of mass  $\mathbf{x}(t)$  [44] for rotating two-component BEC is the same as that for single-component BEC [5]. This ODE system was solved analytically in [44] and different motion patterns of the center were classified in details based on the parameters  $\Omega$ ,  $\gamma_{x,1}$ ,  $\gamma_{y,1}$  and  $\gamma_{z,1}$ .

**Remark 4.1.** When the two shifted centers at  $t = 0$  are different or the trapping potentials are different, i.e.  $\mathbf{x}_1^0 \neq \mathbf{x}_2^0$  or  $V_1(\mathbf{x}) \neq V_2(\mathbf{x})$ , our numerical results show that, in general, there is not such an analytical construction of the solution as in (4.49)–(4.54) for the problem (cf. Figs. 6 and 7).

To verify the analytical solution (4.49) of the CGPEs for rotating two-component BEC, we take  $\Omega = 1$ ,  $\lambda = 0$ ,  $\beta_{11} = 200$ ,  $\beta_{12} = 194$  and  $\beta_{22} = 188$  in (2.9). The initial data in (2.10) is chosen as (4.48) with  $(\phi_1^e(\mathbf{x}), \phi_2^e(\mathbf{x}))$  the central vortex state solution of the CGPEs (2.9) with winding number  $m = 1$ , which is computed numerically by using the same parameters as in dynamics. We consider the dynamics of three different cases:

- (i) with the same traps and the same shifted centers, i.e.  $\mathbf{x}_1^0 = \mathbf{x}_2^0 = \mathbf{x}^0 = (1, 1)^T$  and  $\gamma_{x,1} = \gamma_{y,1} = \gamma_{x,2} = \gamma_{y,2} = 1$ ;
- (ii) with the same traps but different shifted centers, i.e.  $\mathbf{x}_1^0 = (1, 1)^T$ ,  $\mathbf{x}_2^0 = (-1, -1)^T$  and  $\gamma_{x,1} = \gamma_{y,1} = \gamma_{x,2} = \gamma_{y,2} = 1$ ;
- (iii) with the same shifted centers but different traps, i.e.  $\mathbf{x}_1^0 = \mathbf{x}_2^0 = \mathbf{x}^0 = (1, 1)^T$  and  $\gamma_{x,1} = \gamma_{y,1} = 1$ ,  $\gamma_{x,2} = \gamma_{y,2} = 2$ .

Figs. 6, 8 and 9 display the surface plots of  $|\psi_1|^2$  and  $|\psi_2|^2$  at different times for cases (i), (ii) and (iii), respectively. In addition, Fig. 7 depicts the time evolution of the center of mass in (4.49), i.e.  $\mathbf{x}(t)$ , for case (i).

From Figs. 6–9, we can see that (i) when  $\mathbf{x}_1^0 = \mathbf{x}_2^0$  and  $V_1(\mathbf{x}) = V_2(\mathbf{x})$ , the density functions of the two components move like solitary waves in 2D and their shapes do not change during dynamics (cf. Fig. 6) with their mass centers moving exactly in the same way and satisfying the ODE system (4.51)–(4.53) (cf. Fig. 7), confirming the analytical construction (4.49) for the CGPEs (2.9);

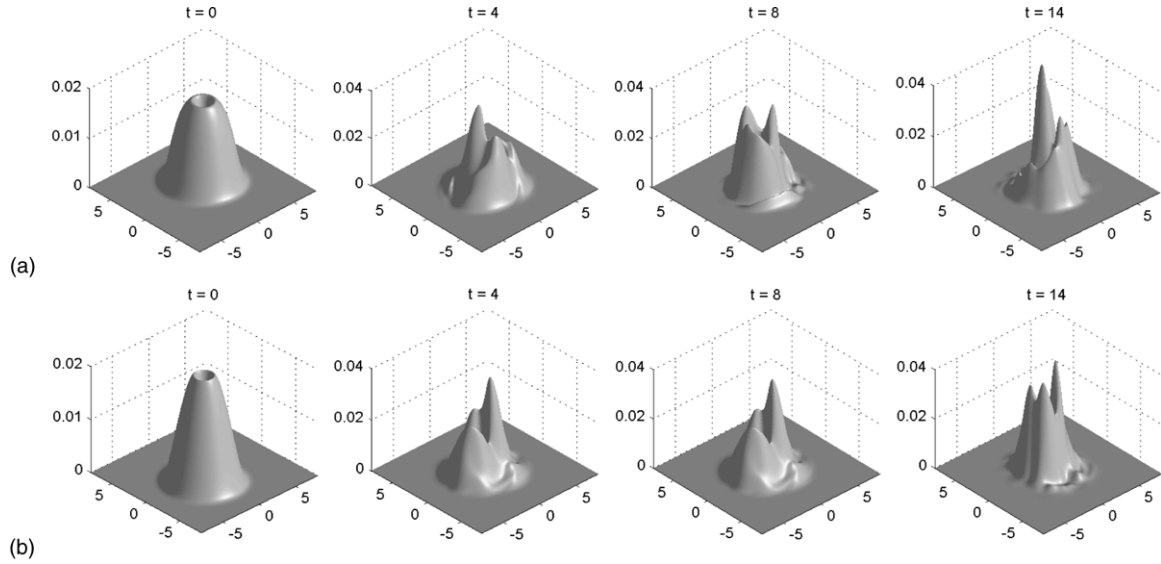


Fig. 8. Surface plots of the wave functions  $|\psi_1|^2$  (top row (a)) and  $|\psi_2|^2$  (bottom row (b)) at different times for case (ii).

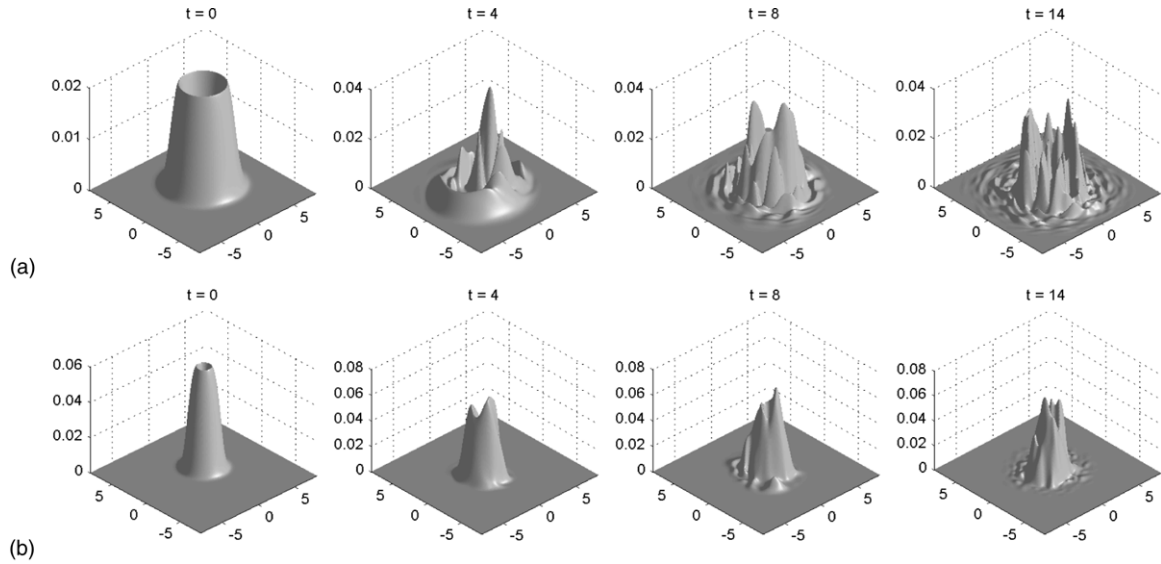


Fig. 9. Surface plots of the wave functions  $|\psi_1|^2$  (top row (a)) and  $|\psi_2|^2$  (bottom row (b)) at different times for case (iii).

(ii) when  $\mathbf{x}_1^0 \neq \mathbf{x}_2^0$  or  $V_1(\mathbf{x}) \neq V_2(\mathbf{x})$ , the dynamics of the two wave functions evolves dramatically (cf. Figs. 8 and 9), suggesting that there may be no soliton-like construction of the solution for rotating two-component BEC in cases (ii) and (iii).

## 5. Conclusion

Based on the coupled Gross–Pitaevskii equations (CGPEs) with an angular-momentum rotation term and an external driving field, we have studied the dynamics of rotating two-component Bose–Einstein condensates (BEC) both analytically and numerically. Along the analytical front, a second-order ODE was derived to describe the time evolution of the density of each component as a periodic function with/without a perturbation, and the frequency of the periodic functions doubles that of the external driving field. We proved the conservation of the angular momentum expectation when the external trapping potentials are radially symmetric in 2D, and respectively cylindrically symmetric in 3D. Another second-order ODE was also derived to describe the time evolution of the condensate width as a periodic function with/without a perturbation, and the frequency of the periodic function doubles the trapping frequency. We also presented an ODE system with complete initial data to govern the dynamics of a stationary state with a shifted center. On the numerical side, we proposed an efficient, accurate and unconditionally stable numerical method for simulating the dynamics of rotating two-component BEC. We also applied the new method to study numerically the dynamics of condensate, including the density of each component, condensate widths, angular momentum expectation as well as quantized vortex lattices and a stationary state with its center shifted from the trap center. In the future, this efficient and accurate numerical method can be

used to study the stability, dynamics and interaction of central vortex states in 2D and 3D for rotating two-component BEC and to make more close comparisons with experimental findings.

## Acknowledgments

We acknowledge support from the Ministry of Education of Singapore grant No. R-146-000-083-112, National Natural Science Foundation of China grant No. 10431060 and Beijing Nova Program grant No. 2005B48. The referees are thanked for their valuable comments, which improved the quality of the paper.

## References

- [1] J.R. Abo-Shaeer, C. Raman, J.M. Vogels, W. Ketterle, Observation of vortex lattices in Bose–Einstein condensates, *Science* 292 (2001) 476–479.
- [2] M.H. Anderson, J.R. Ensher, M.R. Matthews, C.E. Wieman, E.A. Cornell, Observation of Bose–Einstein condensation in a dilute atomic vapor, *Science* 269 (1995) 198–201.
- [3] J.R. Anglin, W. Ketterle, Bose–Einstein condensation of atomic gases, *Nature* 416 (2002) 211–218.
- [4] W. Bao, Ground states and dynamics of multicomponent Bose–Einstein condensates, *Multiscale Model. Simul.* 2 (2004) 210–236.
- [5] W. Bao, Q. Du, Y. Zhang, Dynamics of rotating Bose–Einstein condensates and their efficient and accurate numerical computation, *SIAM J. Appl. Math.* 66 (2006) 758–786.
- [6] W. Bao, D. Jaksch, P.A. Markowich, Numerical solution of the Gross–Pitaevskii equation for Bose–Einstein condensation, *J. Comput. Phys.* 187 (2003) 318–342.
- [7] W. Bao, H. Wang, An efficient and spectrally accurate numerical method for computing dynamics of rotating Bose–Einstein condensates, *J. Comput. Phys.* 217 (2006) 612–626.
- [8] W. Bao, H. Wang, P.A. Markowich, Ground, symmetric and central vortex states in rotating Bose–Einstein condensates, *Comm. Math. Sci.* 3 (2005) 57–88.
- [9] W. Bao, Y. Zhang, Dynamics of the ground state and central vortex states in Bose–Einstein condensation, *Math. Models Methods Appl. Sci.* 15 (2005) 1863–1896.
- [10] C.C. Bradley, C.A. Sackett, R.G. Hulet, Bose–Einstein condensation of lithium: observation of limited condensate number, *Phys. Rev. Lett.* 78 (1997) 985–989.
- [11] S.-M. Chang, W.-W. Lin, S.-F. Shieh, Gauss–Seidel-type methods for energy states of a multi-component Bose–Einstein condensate, *J. Comput. Phys.* 202 (2005) 367–390.
- [12] S.M. Chang, C.S. Lin, T.C. Lin, W.W. Lin, Segregated nodal domains of two-dimensional multispecies Bose–Einstein condensates, *Physica D* 196 (2004) 341–361.
- [13] S.T. Chui, V.N. Ryzhov, E.E. Tareyeva, Phase separation and vortex states in the binary mixture of Bose–Einstein condensates, *J. Exp. Theor. Phys.* 91 (2000) 1183–1189.
- [14] K.B. Davis, M.-O. Mewes, M.R. Andrews, N.J. van Druten, D.S. Durfee, D.M. Kurn, W. Ketterle, Bose–Einstein condensation in a gas of sodium atoms, *Phys. Rev. Lett.* 75 (1995) 3969–3973.
- [15] B.D. Esry, C.H. Greene, J.P. Burke Jr., J.L. Bohn, Hartree–Fock theory for double condensates, *Phys. Rev. Lett.* 78 (1997) 3594–3597.
- [16] J.J. García-Ripoll, V.M. Pérez-García, Stable and unstable vortices in multicomponent Bose–Einstein condensates, *Phys. Rev. Lett.* 84 (2000) 4264–4267.
- [17] J.J. García-Ripoll, V.M. Pérez-García, Split vortices in optically coupled Bose–Einstein condensates, *Phys. Rev. A* 66 (2002) 021602.
- [18] J.J. García-Ripoll, V.M. Pérez-García, V. Vekslerchik, Construction of exact solutions by spatial translations in inhomogeneous nonlinear Schrödinger equations, *Phys. Rev. E* 64 (2001) 056602.
- [19] I. Gasser, P.A. Markowich, Quantum hydrodynamics, Wigner transforms and the classical limit, *Asymptot. Anal.* 14 (1997) 97–116.
- [20] P. Gerard, P.A. Markowich, N.J. Mauser, F. Poupaud, Homogenization limits and Wigner transforms, *Comm. Pure Appl. Math.* 50 (1997) 321–377.
- [21] E.V. Goldstein, M.G. Moore, H. Pu, P. Meystre, Eliminating the mean-field shift in two-component Bose–Einstein condensates, *Phys. Rev. Lett.* 85 (2000) 5030–5033.
- [22] D.S. Hall, M.R. Matthews, J.R. Ensher, C.E. Wieman, E.A. Cornell, Dynamics of component separation in a binary mixture of Bose–Einstein condensates, *Phys. Rev. Lett.* 81 (1998) 1539–1542.
- [23] T.-L. Ho, V.B. Shenoy, Binary mixtures of Bose condensates of alkali atoms, *Phys. Rev. Lett.* 77 (1996) 3276–3279.
- [24] D. Jaksch, S.A. Gardiner, K. Schulze, J.I. Cirac, P. Zoller, Uniting Bose–Einstein condensates in optical resonators, *Phys. Rev. Lett.* 86 (2001) 4733–4736.
- [25] D.M. Jezek, P. Capuzzi, H.M. Cataldo, Structure of vortices in two-component Bose–Einstein condensates, *Phys. Rev. A* 64 (2001) 023605.
- [26] K. Kasamatsu, M. Tsubota, M. Ueda, Vortex phase diagram in rotating two-component Bose–Einstein condensates, *Phys. Rev. Lett.* 91 (2003) 150406.
- [27] K. Kasamatsu, M. Tsubota, M. Ueda, Vortices in multicomponent Bose–Einstein condensates, *Internat. J. Modern Phys. B* 19 (2005) 1835–1904.
- [28] M.-C. Lai, W.-W. Lin, W. Wang, A fast spectral/difference method without pole conditions for Poisson-type equations in cylindrical and spherical geometries, *IMA J. Numer. Anal.* 22 (2002) 537–548.
- [29] C.K. Law, H. Pu, N.P. Bigelow, J.H. Eberly, “Stability signature” in two-species dilute Bose–Einstein condensates, *Phys. Rev. Lett.* 79 (1997) 3105–3108.
- [30] E.H. Lieb, R. Seiringer, Derivation of the Gross–Pitaevskii equation for rotating Bose gases, *Comm. Math. Phys.* 264 (2006) 505–537.
- [31] E.H. Lieb, J.P. Solovej, Ground state energy of the two-component charged Bose gas, *Comm. Math. Phys.* 252 (2004) 485–534.
- [32] T.-C. Lin, J. Wei, Ground state of  $N$  coupled nonlinear Schrödinger Equations in  $\mathbb{R}^n$ ,  $n \leq 3$ , *Comm. Math. Phys.* 255 (2005) 629–653.
- [33] T.-C. Lin, J. Wei, Spikes in two-component systems of nonlinear Schrödinger equations with trapping potentials, *J. Differential Equations* 229 (2006) 538–569.
- [34] K.W. Madison, F. Chevy, W. Wohlleben, J. Dalibard, Vortex formation in a stirred Bose–Einstein condensate, *Phys. Rev. Lett.* 84 (2000) 806–809.
- [35] A. Minguzzi, S. Succi, F. Toschi, M.P. Tosi, P. Vignolo, Numerical methods for atomic quantum gases with applications to Bose–Einstein condensates and to ultracold fermions, *Phys. Rep.* 395 (2004) 223–355.
- [36] E.J. Mueller, T.-L. Ho, Two-component Bose–Einstein condensates with a large number of vortices, *Phys. Rev. Lett.* 88 (2002) 180403.
- [37] C.J. Myatt, E.A. Burt, R.W. Ghrist, E.A. Cornell, C.E. Wieman, Production of two overlapping Bose–Einstein condensates by sympathetic cooling, *Phys. Rev. Lett.* 78 (1997) 586–589.
- [38] L.P. Pitaevskii, S. Stringari, *Bose–Einstein Condensation*, Clarendon Press, 2003.
- [39] H. Pu, N.P. Bigelow, Properties of two-species Bose condensates, *Phys. Rev. Lett.* 80 (1998) 1130–1133.
- [40] F. Riboli, M. Modugno, Topology of the ground state of two interacting Bose–Einstein condensates, *Phys. Rev. A* 65 (2002) 063614.

- [41] B.I. Schneider, D.L. Feder, Numerical approach to the ground and excited states of a Bose–Einstein condensed gas confined in a completely anisotropic trap, *Phys. Rev. A* 59 (1999) 2232–2242.
- [42] D.M. Stamper-Kurn, M.R. Andrews, A.P. Chikkatur, S. Inouye, H.J. Miesner, J. Stenger, W. Ketterle, Optical confinement of a Bose–Einstein condensate, *Phys. Rev. Lett.* 80 (1998) 2027–2030.
- [43] G. Strang, On the construction and comparison of difference schemes, *SIAM J. Numer. Anal.* 5 (1968) 505–517.
- [44] Y. Zhang, W. Bao, Dynamics of the center of mass in rotating Bose–Einstein condensates, *Appl. Numer. Math.* 57 (2007) 697–709.